University of California, San Diego
Institute of Geophysics and Planetary Physics

FINAL REPORT
Contract AF49(638)-1388

Geophysics Division
Air Force Office of Scientific Research
United States Air Force
Washington, D. C.

LOW LEVEL EARTH MOTION

ARPA Order No.	292-69
Program Code No.	9F10
Contract Starting Date:	1 May 1964
Contract Termination Date:	30 September 1969

Project Scientists: Richard A. Haubrich
Principal Investigator

George Backus
Barry Block
Freeman Gilbert
Robert D. Moore
Walter Munk

May 1, 1970
La Jolla, California

Table of Contents

CONSTRUCTING P-VELOCITY MODELS TO FIT RESTRICTED SETS OF TRAVEL-TIME DATA

By George Backus and Freeman Gilbert

Abstract

A scheme recently proposed by the authors for constructing Earth models which fit a given finite set of gross Earth data is applied to the problem of constructing a P-velocity structure which, within experimental error, fits the observed travel times in the range $\Delta = 25^{\circ}(5^{\circ})95^{\circ}$. Three such models are obtained, all of which fit the observed travel times with residuals less than 0.06^{s}, whereas 0.5^{6} is the estimated standard error of the observations. The models differ mainly in the outer 700 km of the mantle.

Bull. seism. Soc. Am. 59, No. 3, pp 1407-1414, June 1969.

INVERSION OF INACCURATE GROSS EARTH DATA

By George Backus and Freeman Gilbert

Abstract

A gross Earth datum is a single measurable number describing some property of the whole Earth, such as mass, moment of inertia, or the frequency of oscillation of some identified elastic-gravitational normal mode. We suppose that a finite set *G* of gross Earth data has been measured, that the measurements are inaccurate, and that the variance matrix of the errors of measurement can be estimated. We show that some such sets *G* of measurements determine the structure of the Earth within certain limits of error except for fine-scale detail. That is, from some sets *G* it is possible to compute localized averages of the Earth structure at various depths. These localized averages will be slightly in error, and their errors will be larger as their resolving lengths are shortened. We show how to determine whether a given set *G* of measured gross Earth data permits such a construction of localized averages, and, if so, how to find the shortest length scale over which *G* gives a local average structure at a particular depth if the variance of the error in computing that local average from *G* is to be less than a specified amount. We apply the general theory to the linear problem of finding the depth variation of a frequency-independent local elastic dissipation (Q) from the observed damping rates of a finite number of normal modes. We also apply the theory to the nonlinear problem of finding density against depth from the total mass, moment and normal-mode frequencies, in case the compressional and shear velocities are known.

Phil. Trans. Roy. Soc. Lond. 266 No. 1173, pp 123-192, 5 Mar 70.

TIDAL TO SEISMIC FREQUENCY INVESTIGATIONS WITH A QUARTZ ACCELEROMETER OF NEW GEOMETRY

By Barry Block and Robert D. Moore

Abstract

A wide-band, tidal to seismic frequency, accelerometer has been developed that is of simple internal geometry and low drift ($<10^{-9}$ *g*/day). Initial tidal and earth-mode frequency investigations are described along with detailed design features and internal noise measurements.

Journal of Geophysical Research, 75, 1493-1505, 1970

EARTH NORMAL MODES FROM A 6.5 MAGNITUDE EARTHQUAKE

(submitted to Nature)

Barry Block

Institute of Geophysics and Planetary Physics, and Physics Department; University of California, San Diego, California

Jay Dratler, Jr.

Institute of Geophysics and Planetary Physics, and Physics Department; University of California, San Diego, California

Robert D. Moore

Institute of Geophysics and Planetary Physics, University of California, San Diego

The earth normal mode spectrum between 8 and 39 cycles per hour (cph) has been obtained with a 20 db signal-to-noise ratio for a relatively small earthquake (M_s = 6.5) using a low noise broad-band vertical accelerometer of new design. The earthquake occurred in the New Hebrides (18°.9 S, 169°.3 E) on October 13, 1969, 06:56 GMT at a depth of 246 kM.

The instrument used[1,2] has a band width extending from tidal to seismic frequencies. It utilizes a quartz fiber in torsion, phase sensitive capacitance detection and electrostatic feedback[3]. The internal instrumental noise was measured in the band 1-30 cph by cross-correlating[2] with another similar instrument, and was found to be the calculated Brownian noise of 2×10^{-24} g^2/cph. Instrumental drift is so small ($< 10^{-9}$ g/day) that operation at full scale tidal gain is possible for several months without re-zeroing.

The instrument has two outputs at present. The tidal output (Fig. 1) is flat from DC to 4.8 cph, where it breaks at 20 db/decade. The gain in the tidal channel is such that $\pm$ 10 volts output, or full scale, corresponds to $\pm$ 3.7×10^{-7}g. The second output is a band pass filter with 40 db gain relative to the tidal channel in a 1-30 cph band. Above 30 cph the filter output drops off at 40 db/decade. The filter gain is such that $\pm$ 10 volts corresponds to $\pm$ 3.7×10^{-9}g in the 1-30 cph pass band. The calibration factor[4] for the instrument was obtained from a static tilt calibration using the tidal data channel and correcting for the added gain of the filter channel in the 1-30 cph passband.

The site, near Miramar Naval Air Station in San Diego, is noisy at seismic frequencies from jet engine noise, but at earth mode frequencies (1-30 cph) the ambient power spectrum (Figs. 3,4) is low enough to permit the measurement of normal mode frequencies and line structure from small earthquakes.

Tidal data for a two day's run is shown in Fig. 1. This is raw data which has been analogue filtered by a two-stage buffered RC filter with a 100 second time constant and digitized at one second intervals. The earthquake (Fig. 2) shows up as a symmetric trace superimposed on the band pass filter record, showing absence of nonlinear mechanical coupling within the instrument. Figures (3,4) show the earthquake power spectrum from 1 to 39 cph. The typical ambient power spectrum of the site was obtained from filter data corresponding to the 15 hour time period AB(Fig. 1). The earthquake power spectrum was obtained from the filter data corresponding to the 15 hour period CD(Fig. 1). The time period BC(Fig. 1) had a small undersea earthquake and could not be used to obtain an ambient power spectrum.

A comparison of the measured modal spectrum with the ambient power spectrum shows that there are several low order modes which can be distinguished[5] from the noise below 10 cph, and that the mode structure above this frequency is real. In fact, in the region from 10 to 39 cph, the signal-to-noise ratio is better than 20 db.

Although not shown in the figures, spectra for both the earthquake and the ambient noise were taken up to a frequency of 120 cph. Up to this frequency, the earthquake spectrum shows considerable structure at least 20 db above the ambient spectrum . At a more favorable site, the ambient noise would be lower and would enable data to be gathered over a longer time for increased mode resolution. For this reason instruments are under construction having a considerably lower Brownian motion limit than the one used here.

The good signal-to-noise ratio (20 dB) found here shows that normal mode and earthquake source data are now obtainable for a far larger class of earthquakes than ever before possible. The smaller earthquakes can be examined for source structure and the large ones, with their consequently longer data runs, can be used to resolve modal line structure. A more complete treatment analyzing several earthquakes is in preparation.

Acknowledgements: The authors wish to thank James Brune for his help in identifying various features of the earthquake, Richard Haubrich for his assistance in the data handling and analysis and Freeman Gilbert for his assistance in identifying normal modes.

This research was supported by the Advanced Research Projects Agency of the Department of Defense and was monitored by the Air Force Office of Scientific Research under Contract No. AF 49(638)-1388.

Captions

Fig. 1. Tidal channel output from 8:29:17 GMT, Oct. 12 to 20:58:36 GMT, Oct. 13. Filter channel output corresponding to tidal data from Section AB was used to obtain the ambient spectrum for the site. The main earthquake time series was taken from the filter channel output corresponding to Section CD.

Fig. 2. Raw filter channel output corresponding to Section CD of Fig(1), showing the details of the time series for the New Hebrides earthquake.

Fig. 3. Spectra from 1 to 14 cycles per hour (cph). The earth normal mode spectrum refers to Section CD in Figs. (1,2). The running mean of the ambient spectrum refers to Section AB in Fig. (1). Brownian motion noise is shown as the heavy solid line. The 0 db point corresponds to an absolute spectral density of 7.4×10^{-25} g^2/cph. Selected modes are identified[5].

Fig. 4. Spectra from 12 to 39 cph. The earth normal mode spectrum refers to Section CD in Figs. (1,2). The ambient spectrum and its running mean refer to Section AB in Fig. (1). Brownian motion noise is shown as the heavy solid line. The 0 db point corresponds to an absolute spectral density of 7.4×10^{-25} g^2/cph. Selected modes are identified[5].

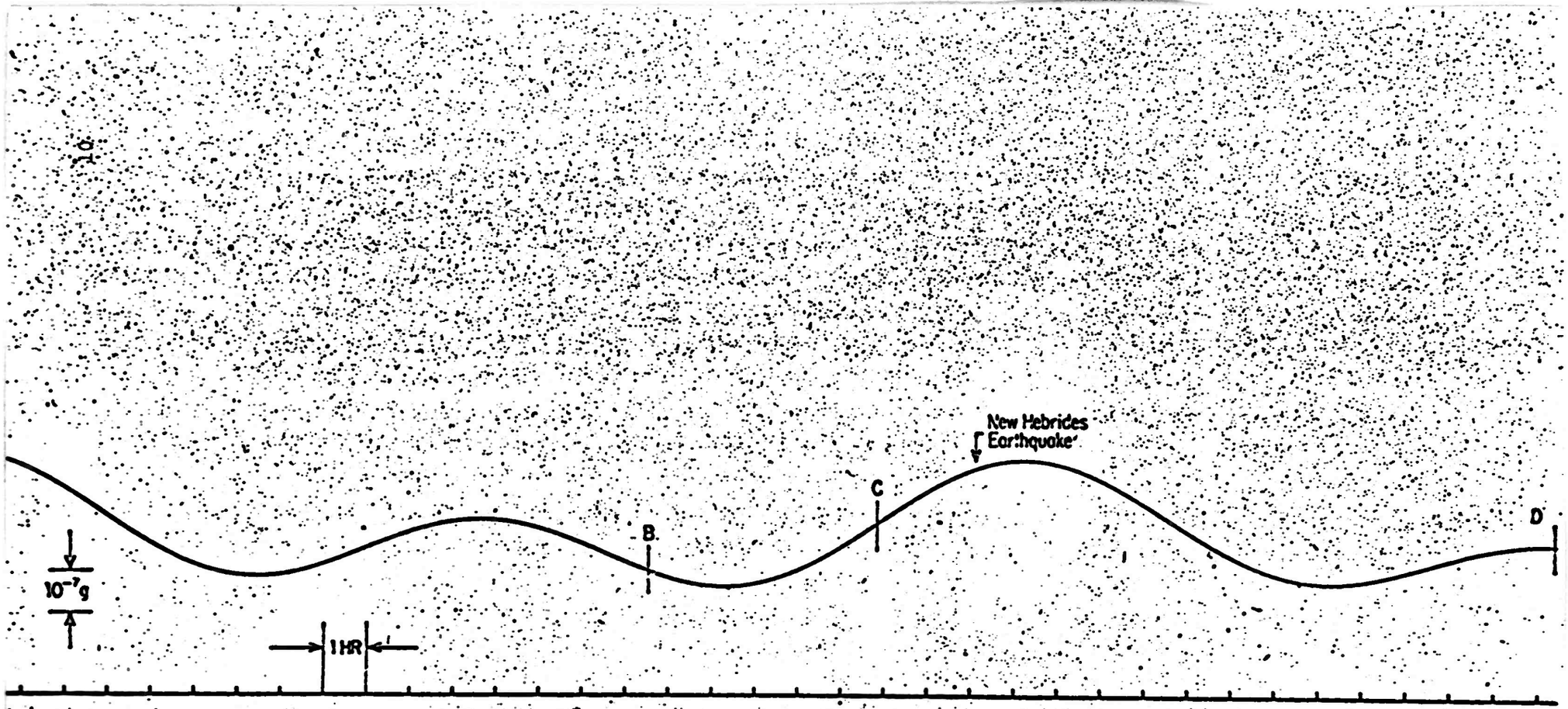

Figure 1

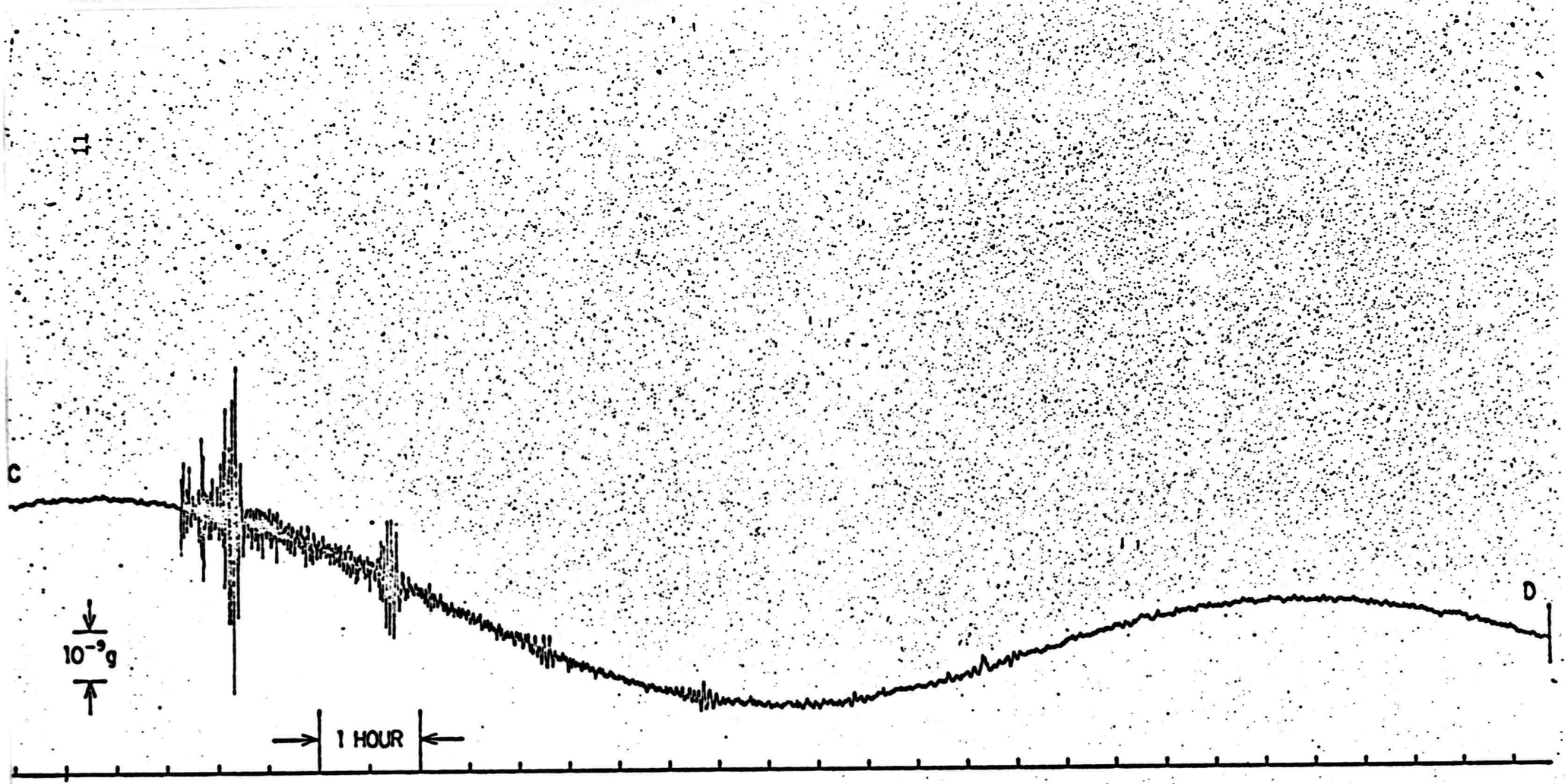

Figure 2

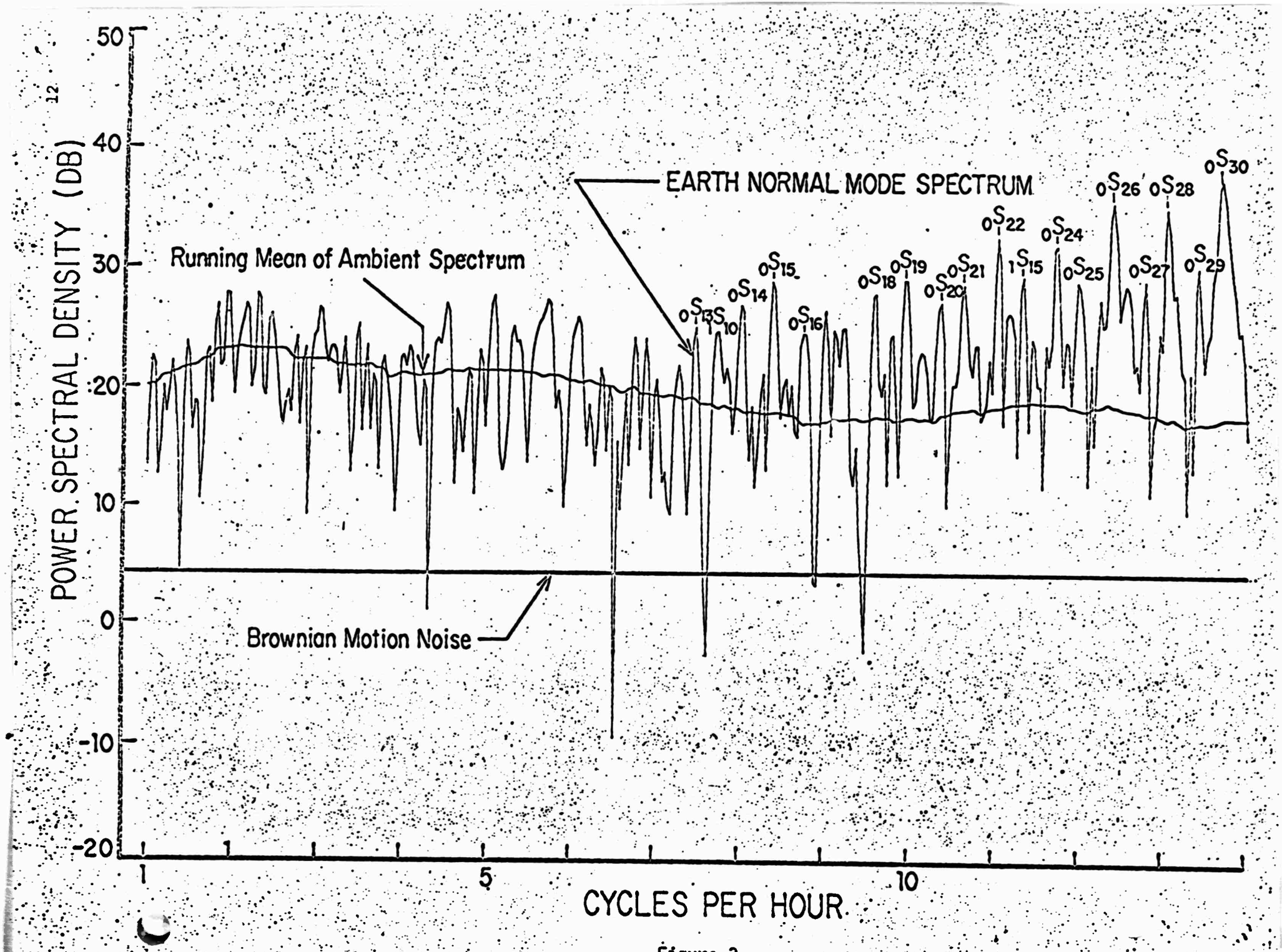
EARTH NORMAL MODE SPECTRUM
Running Mean of Ambient Spectrum
Brownian Motion Noise
POWER SPECTRAL DENSITY (DB)
CYCLES PER HOUR
50
40
30
20
10
0
-10
-20
1
5
10
0S13 S10
0S14
0S15
0S16
0S18
0S19
0S20
0S21
0S22
1S15
0S24
0S25
0S26
0S27
0S28
0S29
0S30

Figure 3

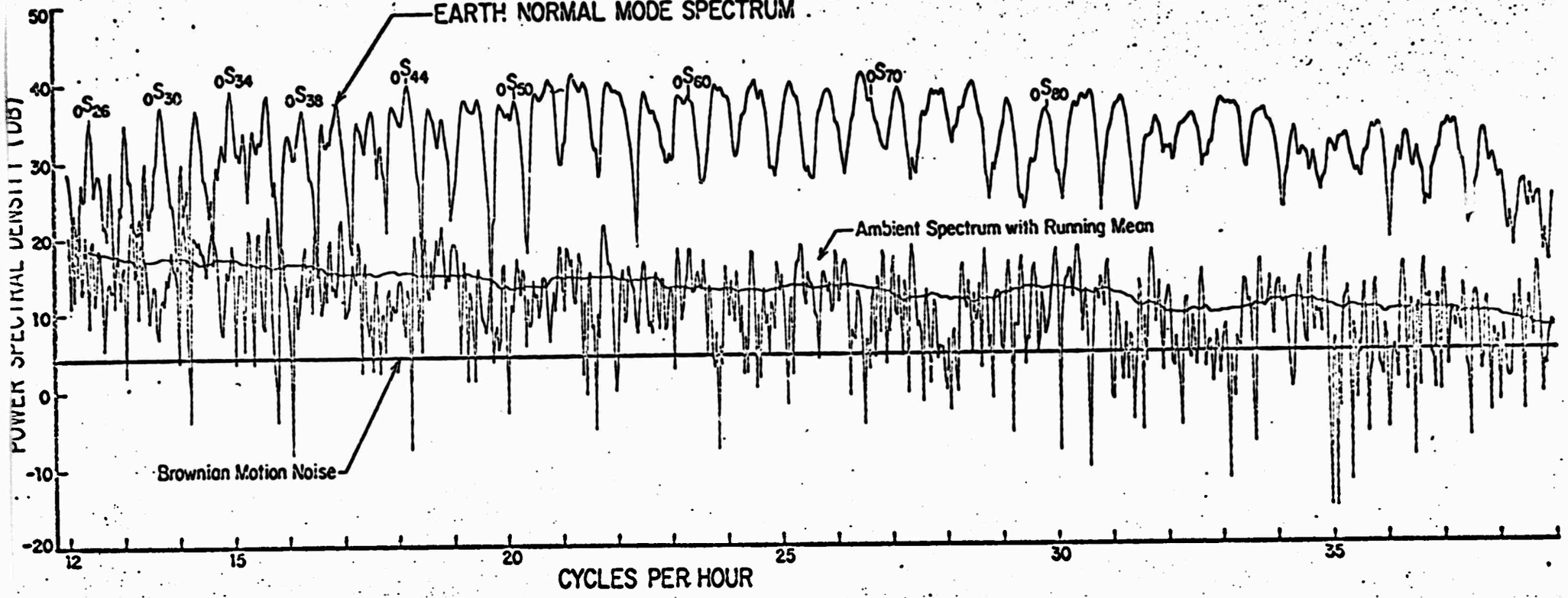
EARTH NORMAL MODE SPECTRUM
$_0S_{26}$
$_0S_{30}$
$_0S_{34}$
$_0S_{38}$
$_0S_{44}$
$_0S_{50}$
$_0S_{60}$
$_0S_{70}$
$_0S_{80}$
Ambient Spectrum with Running Mean
Brownian Motion Noise
POWER SPECTRAL DENSITY (DB)
50
40
30
20
10
0
-10
-20
12
15
20
25
30
35
CYCLES PER HOUR

Figure 4

References

1. B. Block, R. D. Moore, Transactions, American Geophysical Union 50, No. 4, April 1969.
2. B. Block, R. D. Moore, Tidal to Seismic Frequency Investigations with a Quartz Accelerometer of New Geometry. J. Geophys. Res. (in press).
3. B. Block, R. D. Moore, Measurements in the Earth Mode Frequency Range by an Electrostatic Sensing and Feedback Gravimeter, J. Geophysical Res., 71, 4361-4375 (1966).
4. W. E. Farrell, R. D. Moore, Linearization and Calibration of Modified LaCoste Gravity Meters. J. Geophys. Res. (in press).
5. Freeman Gilbert, private communication and G. Backus and F. Gilbert, Uniqueness in the Inversion of Inaccurate Gross Earth Data. Phil. Trans. Roy. Soc. Lon. A, in press, (1970).

MICROSEISM MEASUREMENTS ON THE DEEP OCEAN BOTTOM

By Hugh Bradner

Abstract

Several laboratories have developed apparatus for ocean-bottom seismic measurements and have made a total of about 200 records in deep oceans. They have observed earthquakes, measured propagation velocities, studied microseism noise, and determined that signal-to-noise ratios may allow them to monitor bomb tests. But many more measurements will be needed before definitive generalizations can be made about the generation and attenuation of microseisms.

Nautilus, 4, (1968)

OCEAN MICROSEISM MEASUREMENTS WITH A NEUTRAL BOUYANCY FREE-FLOATING MIDWATER SEISMOMETER

H. Bradner, Louis G. de Jerphanion* and Richard Langlois**

Institute of Geophysics and Planetary Physics
University of California, San Diego

ABSTRACT

Seismometers in spherical aluminum pressure housings have been weighted to float stably at midwater depths in the ocean, and thus record water motions in a frequency band of 0.02 to 5 cps. Simultaneous records made with a midwater instrument at 1.2 km depth and a bottom instrument at 4.6 km depth showed coherence at spectral power peaks of leaky organ pipe frequencies, and additional coherence peaks at frequencies down to 0.025 cps. Twenty organ pipe modes can be tentatively identified. The spectral power can be attributed almost entirely to microseismic motions in waveguide modes. We conclude that the forcing functions for microseisms are broad enough so that deep ocean bottom and midwater microseism spectral peak frequencies are characteristic of local bathymmetry.

* Present address: Intertechnique, 78 Plaisir, Paris France

** Present address: Department of Chemistry, Columbia University Graduate School.

1. INTRODUCTION

We have modified our ocean-bottom seismometers to be neutrally bouyant at predetermined depths in the ocean, like Swallow floats.[1] Such stable midwater operation is possible since the aluminum pressure cases of our instruments are less compressible than sea water. The work was initially undertaken by the first and third authors in order to study the modes of ocean waveguide excitation that had been inferred from ocean-bottom seismic background spectra.[2] The second author joined the work as a master's degree thesis project. Additional motivation for the work arose from our belief that water motion around ocean-bottom instruments may mask seismic background spectra at frequencies lower than the microseism peak. A free-floating neutrally buoyant instrument will move almost exactly as the surrounding water and hence will not produce signals due to steady water flow. The correspondence is not quite exact because the compressibility of the instrument is not the same as water. The center of mass of the instrument is displaced from the geometrical center, and the seismometer has a small spring-supported mass which moves with respect to the center of mass of the instrument.

Section 2 of the present paper will review briefly the theory of waveguide mode excitation. Section 3 will describe the instruments. Section 4 will consider the motion of a neutrally buoyant instrument in a moving medium. Finally, section 5 will discuss some experimental results.

2. OCEAN WAVEGUIDE MODES

The general equation for the displacement potential of small amplitude elastic wave motion in a homogeneous fluid is the simple wave equation

$$\frac{\partial^2 \psi}{\partial t^2} = c^2 \frac{\partial^2 \psi}{\partial x^2}$$

If we consider a source to be an antinode of pressure oscillations on a rigid bottom interface, and consider the air above the top interface to be massless, we can write the solution of the wave equation as a plane wave

$$\psi = 2A \sin(2\pi ft) \sin(2\pi x/\lambda)$$

with wavelength $\lambda = 4H/(2n + 1)$, where x is the depth of observation and H is the water depth. This model would predict "organ-pipe" resonant modes in the ocean waveguide. More realistic models with distant sources and semirigid layered bottoms lead to a somewhat similar mode structure, although the frequencies are not always exact multiples of the fundamental; and they may show different excitation amplitudes; and there is not an amplitude node at the ocean bottom for most modes. (See for example Chapter 4 of Ewing, Jardetzky and Press[3].

Abramovici computed the modes for a layered bottom.[4] He shows that these modes reproduced in Fig. 1 are in good agreement with measured ocean-bottom power spectra.[2] In all cases, the water surface is a displacement antinode. Hence the ratio of midwater

power to bottom power in vertical organ pipe modes can be written readily as:

$$\frac{\cos^2 2\pi fx/c}{\cos^2 2\pi fH/c}$$

where f is the frequency of the leaky organ pipe mode, x is the depth of the midwater observation, H is the water depth, and c is the velocity of compressional waves in water. The power ratio for modes other than vertical organ pipe generally cannot be expressed in this simple form.

3. INSTRUMENTS

The basic instruments were our ocean-bottom seismometers, consisting of California Institute of Technology/United Electrodynamics 1-cps lunar velocity transducer seismometers in orthogonal triaxial arrangement with tape recorders in 65-cm-diameter aluminum pressure cases.[2] For midwater use, the anchor was replaced by a counterweight of the proper net weight to make the instrument float at a predetermined depth in ocean water. The counterweight was attached in a manner similar to the anchor of the ocean-bottom instrument, and was released at a predetermined time by electrolytic solution of a magnesium pin. A supplementary weight of approximately 10 kg was employed to sink the instrument rapidly to near the desired operating depth, where this weight was released by the bursting of a calibrated diaphragm. A pressure transducer was mounted on the instrument to record its depth on a Rustrack recorder or on one frequency-modulated track of the magnetic tape recorder. A three-component instrument is shown schematically in Fig. 2.

4. MOTION OF A NEUTRALLY BUOYANT INSTRUMENT

When the instrument is near its equilibrium depth in still water, its free oscillatory motion is characterized by the float compressibility and the Väisälä frequency.[5] (The float frequency is slightly higher than the Väisälä frequency.) The accelerations associated with this damped motion below the thermocline are negligible within the 0.02 - 5 cps pass band of our instruments. If the center of mass of the instrument were at its center of buoyancy, and if no interior parts were flexibly mounted, then after reaching equilibrium depth, the instrument would follow all nonrotational or shear-free motions of the water in our pass band. Since the center of mass hangs directly below the center of buoyancy, and the seismometer mass is negligibly small we can say with adequate validity that the instrument follows the vertical water motion. Water motion due to compressional waves can be considered shear-free in our observations, since the wavelength is very much larger than the dimensions of the instrument.

Horizontal water motion can produce seismometer signals by rocking the instrument with moderately low damping at its natural rocking frequency. This frequency is a function of the moment of inertia and the location of the center of mass; and in our instruments produced a discernible spurious power peak at 0.39 ± 0.01 cps in water tank tests. The rocking oscillations were less violent in the ocean experiments, and were unobservable in an experiment at 1210 m. depth.

The release of the counterweight is accomplished through the electrolytic etching of a magnesium pin. This produces an effective change in instrument buoyancy of 0.3 gm in 4 hours. Since 1 gm change in buoyancy

causes a 3-meter change in equilibrium depth the dissolving magnesium produces a small average vertical velocity of 6.25×10^{-3} cm sec^{-1}. Accelerations associated with this average velocity should be negligibly small.

We believe therefore that the midwater instrument gives a valid indication of water motion in the frequency range from 0.02 to 4 cps. The main motion is expected to be due to compressional waves, though the ocean is a stratified fluid with unknown flows that can also arise from internal waves and driven motions. The frequencies of internal waves are expected to lie outside our passband but we cannot exclude a'priori the possibility of spurious signals from unknown driving forces.

5. EXPERIMENTAL RESULTS

Near-Shore Observations

Station 2 was run in water depth of 1500 ± 50 m over broken bottom at a location 24 km southwest of San Diego. Throughout a four-hour period the instrument stayed at a constant depth of 430 m within the resolution of the depth recorder (±40m).

Station 4 was run in the same water depth, within 10 km of Station 2. The instrument depth was 800 ± 40 m. The two runs were separated in time by seven months. Original analog magnetic tape records were digitized on an Adage computer, using time markers that had been recorded on the tape during the seismic measurements. The digitized records from the three-component triaxial seismometers were rotated during spectral analysis on a CDC digital computer to yield vertical and horizontal spectral power densities and coherences.

Fig. 3 shows the vertical spectral from the two observations. The apparent peak in power density at 0.34 cps is due to the natural rocking period of the instrument, and prevents a comparison between the spectra between about 0.3 and 0.5 cps. The spectra outside of this band show several common power peaks, (see Table I), implying that the microseism background may have a peaked structure whose frequencies are characteristic of the bathymmetry, and whose amplitudes are indicative of a non-white forcing function. The frequencies of leaky organ-pipe modes have not been calculated for this geographic region.

Deep Water Observations

The midwater seismic measurement of Station 5 was a 16 hour record in water of 4.6 km depth over a uniform bottom at a location 78 km north of Oahu, Hawaii (Fig. 4). A south-southwest moving swell ran 2 to 4 meters high during the experiment. The three-component triaxial seismometer floated at a depth of 1210 m ± 40 m. A simultaneous record was made on the uniform flat bottom with a similar instrument. The instruments were equipped with low-noise Texas Instrument Company parametric amplifiers, and the 1-cps seismometers were low-pass filtered at 0.1 cps.

Qualitative comparison can be made between the spectral structure observed in this experiment, at 22°, 25'N, 158°, 08'W (location by sextant) and the spectral structure observed four years earlier with a bottom seismometer at a nearby location, 22°, 28'N, 158°, 00'W. The spectrum from the earlier observation is reproduced here as Fig. 5. The upper frequencies in the spectrum from the present experiment are supressed by the low-pass filter, so that the spectrum is not unambiguously discernable above background for frequencies higher than 1 cps. However, the midwater vs. bottom coherence peaks discussed later (Fig. 10) indicate that the mode structure continues

out to at least 4 cps and has similar peak frequencies during both observations. Four sections of data were analyzed: the first record started 6 hours after the bottom instrument was launched. Additional two hour length records were analyzed from 0 to 4 cps from midwater and bottom instruments, beginning at 10 hours, 14 hours and 18 hours after launching the bottom instrument. Both instruments showed small changes in spectral power distribution during the recording time, though the peak frequencies did not change.

Figure 6 shows the X, Y and Z spectra from the midwater instrument out to 4 cps during the last recording interval. The spectra have been displaced vertically in the figure for clarity: The power density between 2 and 4 cps is very nearly the same for each component. Figure 7 is a similar display for the bottom instrument. The spectral shapes from the two instruments are strikingly similar and show apparent resonance peaks in vertical power.

Figures 8 and 9 show higher resolution spectra from the two instruments below ½ cps during the last recording interval. The pronounced peaks at 0.05, 0.1 and 0.2 cps in the MWS record are not clearly evident in the bottom record.

for station 5

In all instances the time series consisted of 7200 terms, beginning at 18 hours. Thus the 4 cps records and the ½ cps records were analyzed during overlapping but not identical times. Information on the statistical parameters for the power spectra at all stations is given in Table II.

A large persistent power difference between X and Y in the 0.1 cps peak during the analyses at ½ cps implies that the midwater seismometer turned through about 45° during the 16 hour period.

Sections of the original analog records were examined on a Panoramic RTA-5 Spectrum Analyzer to determine that the observed spectral shape and peak structure were valid, and were not artifacts produced by the digital analysis.

Figure 10 shows the vertical component spectra from the two instruments, and their coherence. In this figure the spectra have not been displaced vertically; they indicate true relative power in the midwater and bottom vertical motions.

High resolution calculations of relative amplitude, coherence and phase between X, Y and Z components of the MWS record show that the 0.05 cps peak is a vertically moving compressional wave, while the 0.1 cps peak comes from horizontal motion. The power density in the 0.05 cps peak of the MWS is two orders of magnitude greater than the bottom, while the power density in the 0.1 cps peak is one order of magnitude greater than the bottom. Another small peak in the MWS record at 0.35 cps shows greater than 95% confidence coherence with the bottom record. The 0.05, 0.1 and 0.35 cps coherent peaks represent high Q waveguide excitation modes which we feel are characteristic of the physical environment rather than peaks in a forcing function.

The weak signal at frequencies above 1 cps makes coherence low. However if we tabulate all well defined vertical power coherent peaks regardless of size we find remarkably close agreement with the frequencies of leaky organ pipe modes calculated by Abramovici. See table III. By looking at only the vertical coherence we will overlook other possible modes, and the agreement with organ-pipe modes may be illusory.

High resolution analysis showed that there is no power peak at 0.09 cps corresponding to the fundamental organ pipe mode (Fig. 8). The high coherence peak at 0.10 cps was shown by amplitude and phase comparison to be almost entirely horizontal X motion. The 0.05 cps peak which may have significant coherence with the bottom record, is almost entirely Z motion. The incoherent peak at 0.20 cps is horizontal with equal power in X and Y.

Vertical power coherence is high at 0.35 and at 0.45 cps though no power peak shows above the background at 0.45 cps.

By calculating spectral coherences and phases with shifted start times on the MWS time series, we found indication that the bottom seismometer lagged approximately 3 sec behind the MWS, thus supporting the idea that we are observing modes whose energy flows downward past the floating instrument toward the bottom. We were also able to determine that the high frequency spatial coherence dimished rapidly for shifts greater than about 8 sec thus indicating that the waveguide Q plus the forcing function for $\approx$ 4 cps waves has a time-coherence of about 30 cycles. Similar measurements on the 0.10 cps peak show that its time coherence is greater than 40 cycles (400 sec), while the peak at 0.35 cps has a time coherence between 72 and 144 cycles (200-400 sec).

We are unable to make direct test of organ-pipe modes by comparing midwater power with bottom power at the coherent peaks, since the signal/noise ratio was severely reduced by the low-pass filter. We attempted to make a qualitative test by arguing that coherence will be reduced wherever the term $\cos^2 2\pi fx/c$ or $\cos^2 2\pi fH/c$ is small. The agreement appeared qualitatively valid above 2 cps but was not conclusive.

On the basis of all our experimental data we conclude that the seismic background at frequencies up to at least 4 cps may be carried in well defined waveguide modes where the bottom is uniform over a distance of several wavelengths. Leaky organ-pipe modes are probable. Abramovici has obtained a good theoretical fit to our 1963 data by assuming a white forcing function. However our additional data indicate that an uneven and time-varying forcing function is operative. Alternatively we might say that the generating zone of microseisms according to the model of Haubrich[6] can be characterized by waveguide modes, especially leaky organ-pipe modes,

with a non-white forcing function. This is in agreement with earlier ocean bottom three-component seismic records which indicated organ-pipe modes near land masses, converting to Rayleigh waves at greater distance from shore[7].

ACKNOWLEDGEMENTS

We wish to thank the many members of IGPP for their counsel and help.

This research was supported by the Advanced Research Projects Agency of the Department of Defense and was monitored by the Air Force Office of Scientific Research under Contract No. AF 49(638)-1388.

REFERENCES

(1) Swallow, J.C., A Neutral-buoyancy Float for Measuring Deep Currents, *Deep Sea Res., 3,* 74-81, (1955).

(2) Bradner, H. and Dodds, J.G., Comparative Seismic Noise on the Ocean Bottom and on Land, *J. Geophys. Res., 69,* 4339-4338 (1964).

(3) *Elastic Waves in Layered Media,* Ewing, Jardetzky and Press, McGraw Hill, 1957.

(4) Abramovici, F., Diagnostic Diagrams and Transfer Functions for Oceanic Wave-Guides, *Bull. Seis. Soc. Am., 58,* 427-456 (1968).

(5) The Väisälä frequency is a measure of the adiabatic oscillation stability of a small mass of fluid. See for example Eckart, *Hydrodynamics of Oceans and Atmospheres.* Pergamon, London, 1960; M.V. Hill, *The Sea Vol. I,* Interscience, 1962.

(6) Haubrich, R.A., W.H. Munk, and F.E. Snodgrass, Comparative Spectra of Microseisms and Swell, *Bull. Seis. Soc. Am., 53,* 27-37 (1963).

(7) Bradner, H., J.G. Dodds, and R.E. Foulks, Investigation of Micro-seism Sources with Ocean Bottom Seismometers, *Geophysics, 30,* 511-526 (1965).

FIGURE CAPTIONS

Figure 1 (Reproduced from Abramovici[4])

Power density spectrum P on ocean bottom, January 21, 1963 (Bradner and Dodds, 1964). Location: 22° 28'N, 158° 00'W. The isolated points show peaks of the transfer function T for Hilo 31 with the attenuation factor $A = e^{-(0.002F_i/g)}$. The scales for P (left) and T (right) are logarithmic.

Figure 2 Schematic view of Midwater Seismometer three-component triaxial seismometer is contained in aluminum pressure housing, along with amplifiers, crystal clock, tape recorder and radio recovery beacon transmitter.

Figure 3 Comparison of Vertical Power Spectram for Midwater Seismometer, Stations 2 and 4.

Figure 4 Bathymmetry in vicinity of Station 5.

Figure 5 (Reproduced from Bradner and Dodds[2]). Seismic background spectra on land and ocean bottom, February 8, 1963, Hawaii. The land instrument was a vertical seismometer. The ocean-bottom instrument contained three-component equiaxial seismometers. Only one component is displayed. The other two components were similar. The scales at the top of the figure show the frequencies of organ-pipe modes in the water.

Figure 6 Horizontal and Vertical Power Spectra to 4 cps. Midwater Seismometer, Hawaii Station 5. The plots have been displaced vertically by different amounts for clarity. Actual X: Y: Z power densities averaged over the range 2-4 cps are in the ratio 1: 1.20: 1.10.

TABLE I

Peaks in Vertical Spectrum, Stations 2 and 4.

Frequency (cps)	
Stn 2	Stn 4
0.25	0.27
0.55	0.55
0.95	(0.9)
(1.35)	
(1.6)	1.55
(1.75)	
	1.9
2.1	2.2
	2.4
	2.6
2.75	
	3.2
3.65	
3.85	3.85
	(4.1)
4.35	4.35

TABLE II

Time Series Used in Calculating Power Spectra in this Paper

Fig.	St'n	Series length (minutes)	No. terms	Samples/sec	No. lags	No. deg. freedom
3	2	3 3/4	4107	18.2	180	46
	4	6	6479	18.2	180	72
5	-	8	8648	18	200	90
6	5	15	7200	8	100	144
7	5	15	7200	8	100	144
8	5	120	7200	1	100	144
9	5	120	7200	1	100	144
10	5	15	7200	8	100	144

TABLE III

Frequencies of Observed Power Peaks Compared with

Frequencies of Abramovici's calculated Modes. Station 5.

Mode	Frequency (cps)	
	Abramovici(1)	Observed(2)
1	0.09	0.08*
2	0.25	0.26
3	0.42	0.45
4	0.58	0.64
5	0.73	0.72
6	0.78	0.88
7	0.93	
8	1.08	1.08
9	1.14	1.20
10	1.28	1.32
11	1.45	1.52
12	1.62	1.64
13	1.78	1.76
14	1.95	1.90
15	2.12	2.08
16	2.29	2.20
17	2.45	2.32 2.52
18	2.62	2.64
19	2.78	2.76
20	2.93	2.92

(1) Frequencies were read from Abramovici's plots and are uncertain to about ±0.01 cps below mode 10, and about ±0.02 cps in the higher modes.

(2) Observed frequencies were determined by peaks in coherence between NWS and BOT instruments. Peak position accurate to ±0.02 cps. (See Fig. 12)

---

* Higher resolution analysis shows that the high coherence peak occurs at 0.10 cps; and there may be also statistically significant peaks around 0.05 and 0.36 cps.

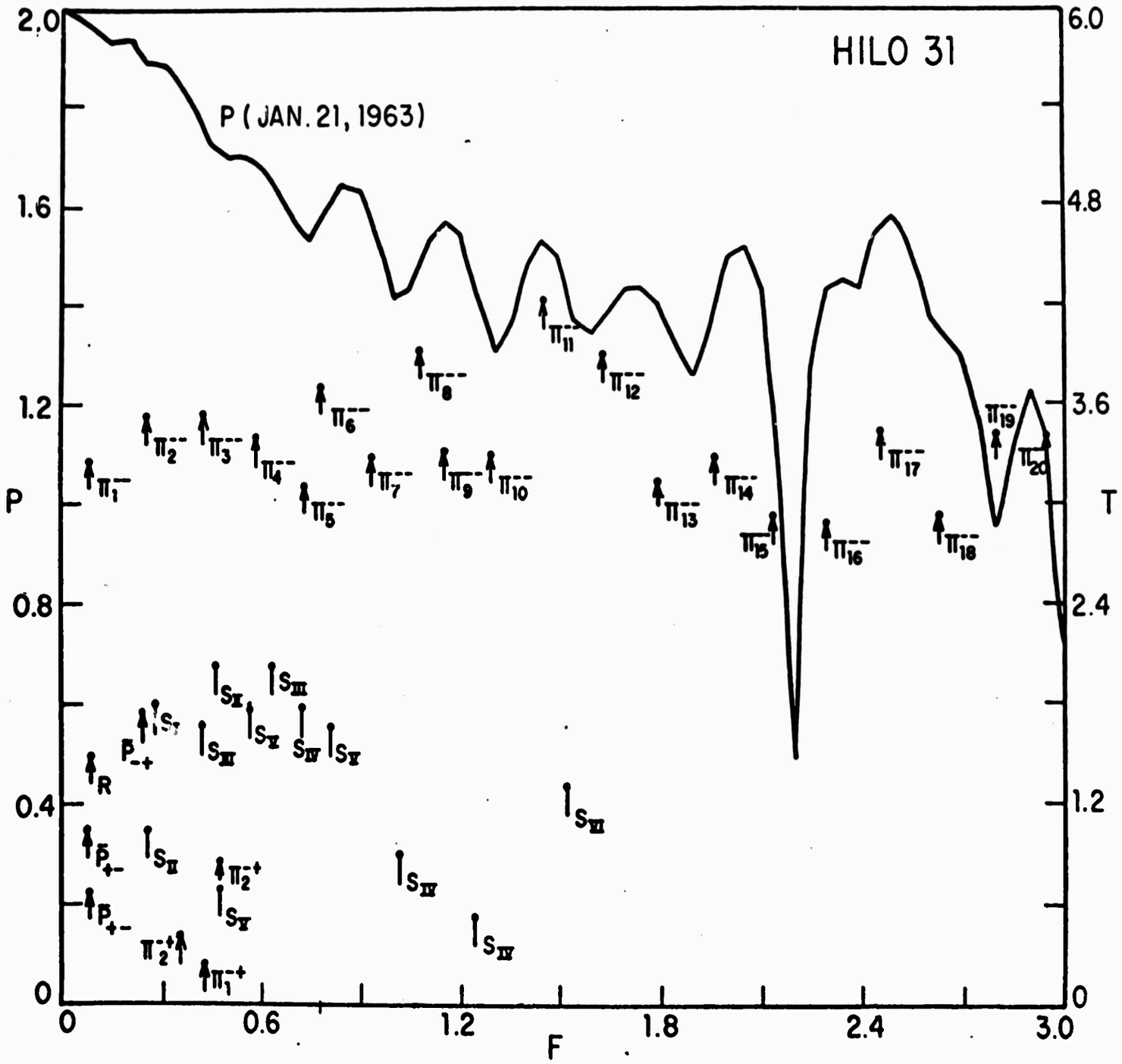
HILO 31
P (JAN. 21, 1963)
P
T
F
2.0
1.6
1.2
0.8
0.4
0
6.0
4.8
3.6
2.4
1.2
0
0.6
1.2
1.8
2.4
3.0

Fig. 1

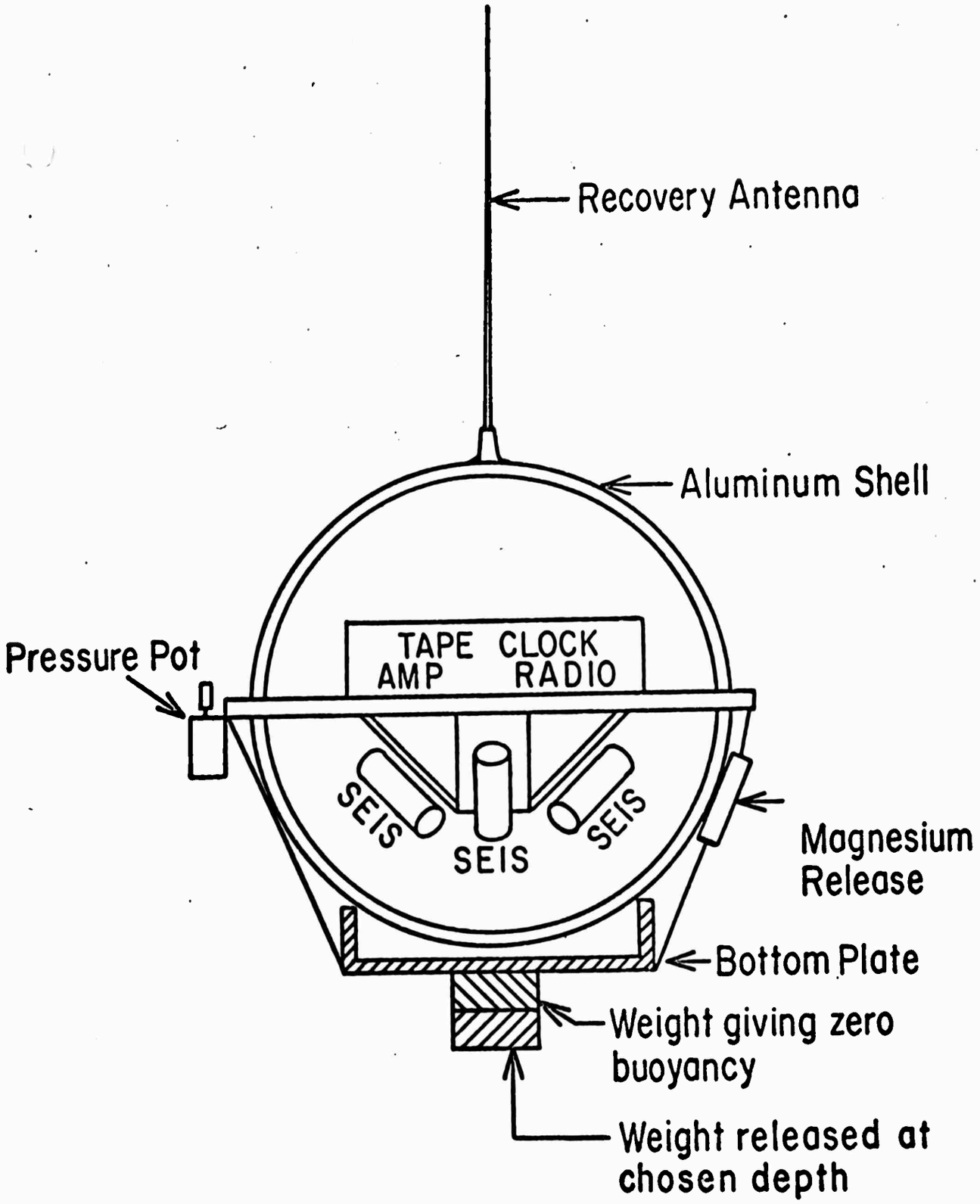

Figure

Schematic View of the Midwater Seismometer

Fig 2

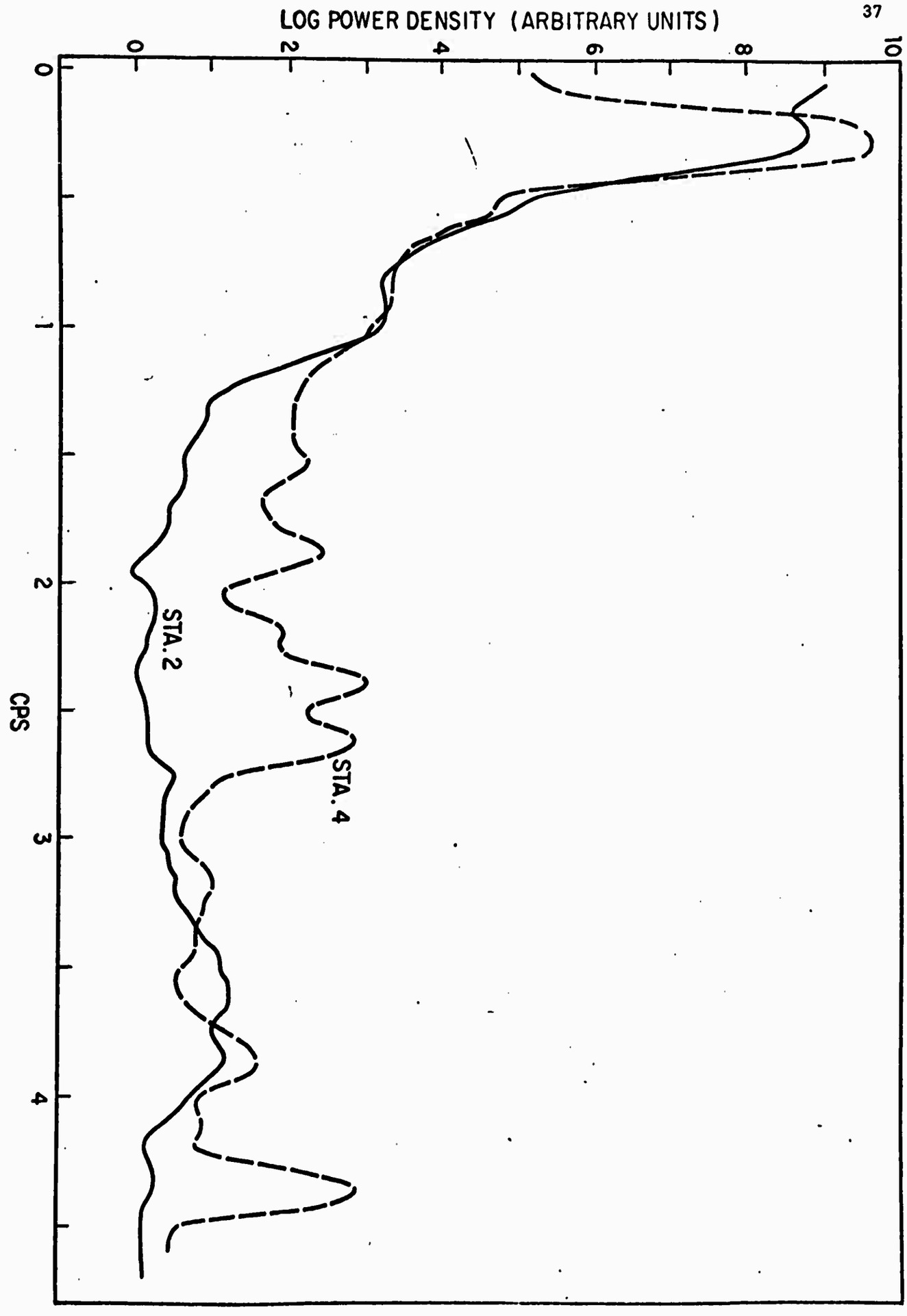
LOG POWER DENSITY (ARBITRARY UNITS)
0
2
4
6
8
10
0
1
2
3
4
CPS
STA. 2
STA. 4

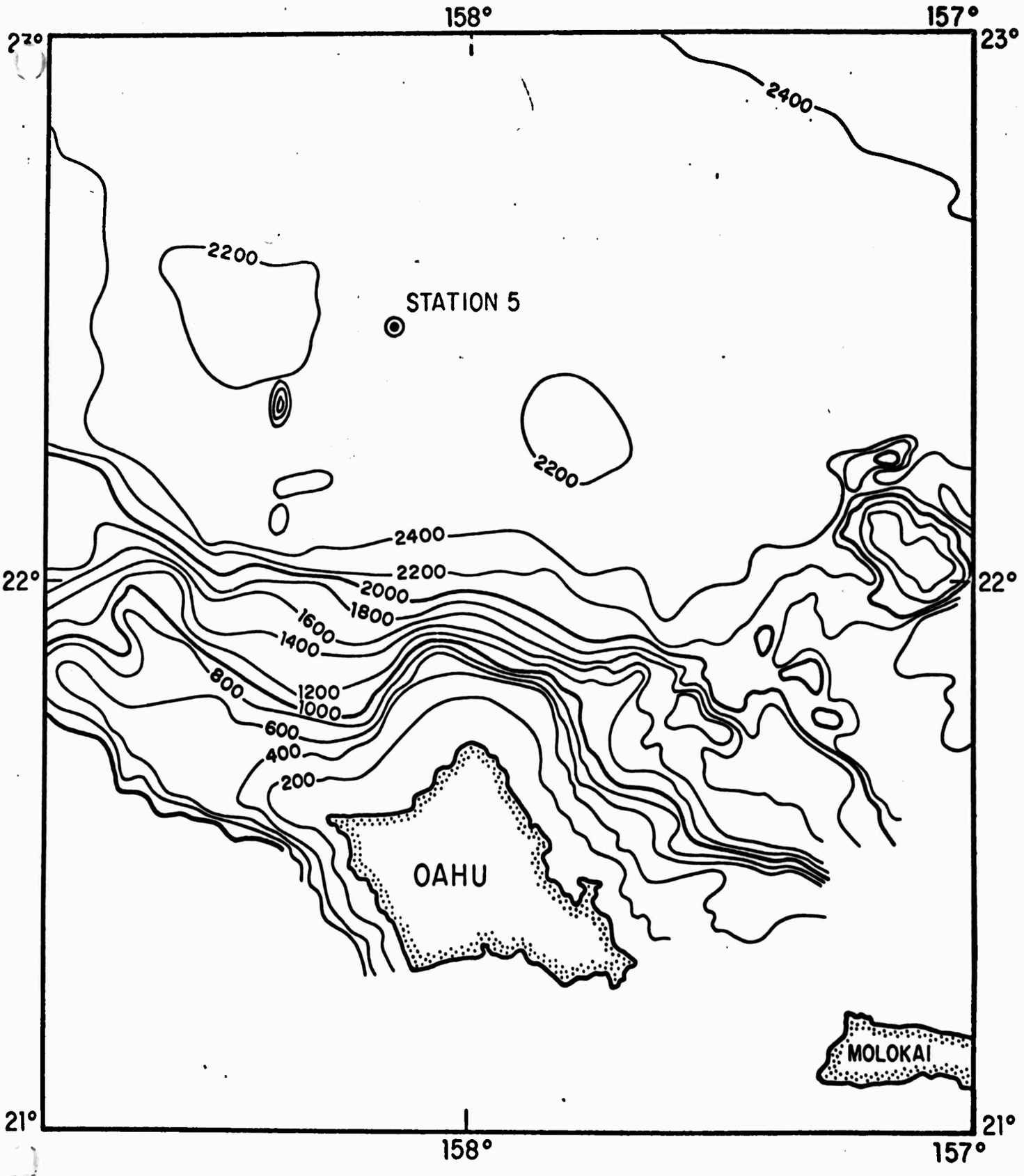
158°
157°
23°
22°
21°
2400
2200
STATION 5
2200
2400
2200
2000
1800
1600
1400
1200
1000
800
600
400
200
OAHU
MOLOKAI

Fig 6

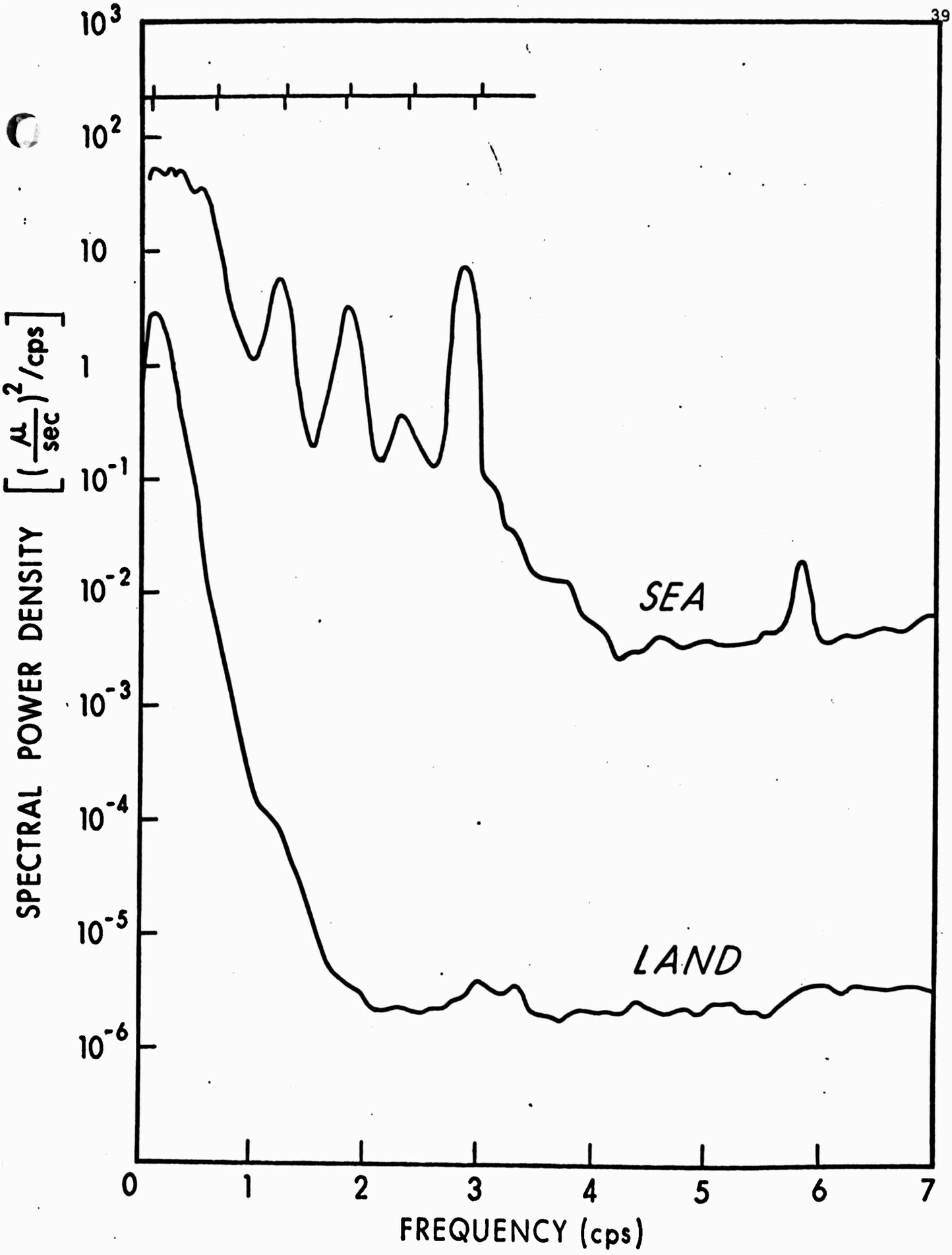
SPECTRAL POWER DENSITY $\left[\left(\frac{\mu}{sec}\right)^2/cps\right]$
10^3
10^2
10
1
10^{-1}
10^{-2}
10^{-3}
10^{-4}
10^{-5}
10^{-6}
SEA
LAND
0
1
2
3
4
5
6
7
FREQUENCY (cps)

Fig. 5

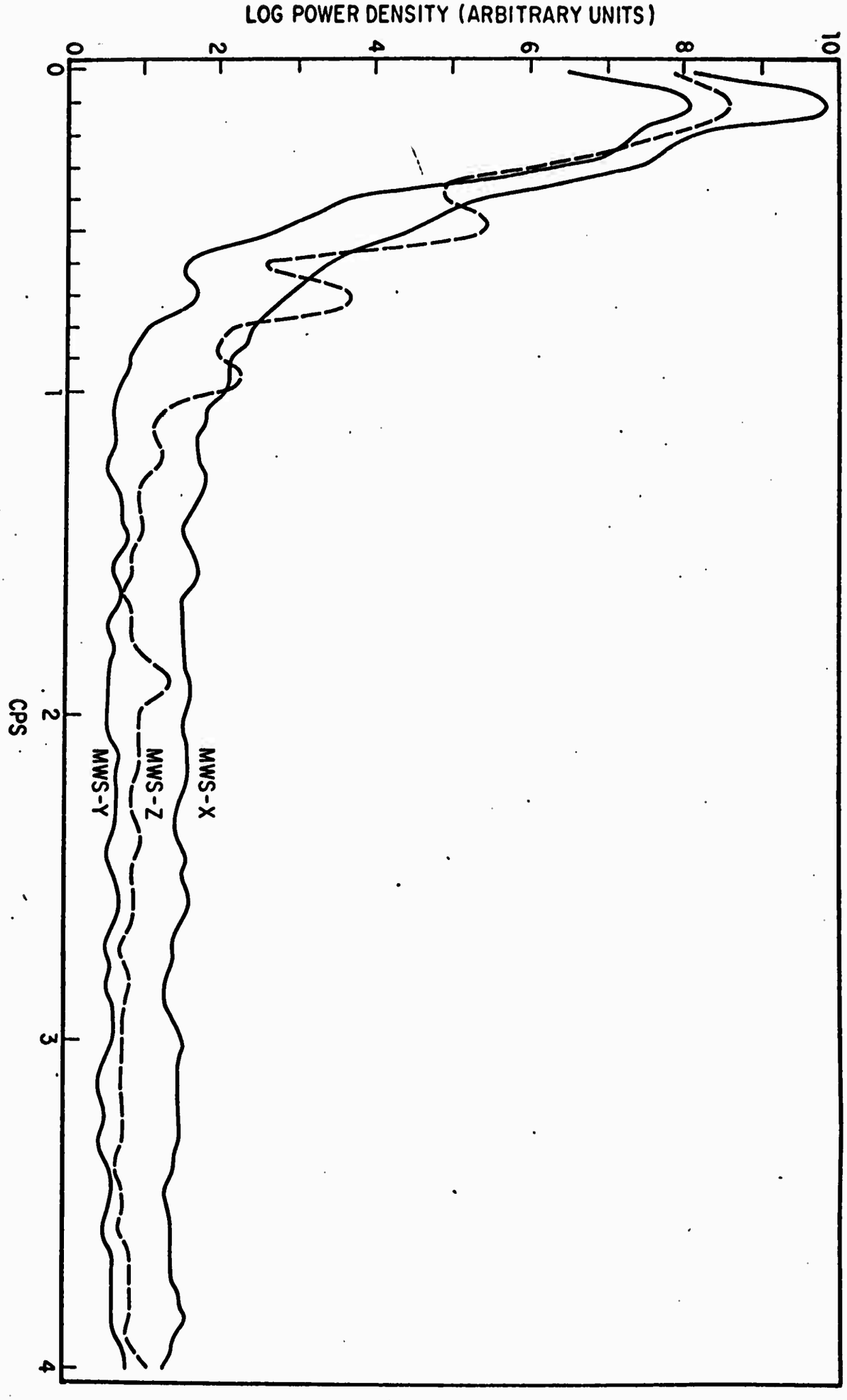
LOG POWER DENSITY (ARBITRARY UNITS)
0
2
4
6
8
10
0
1
2
3
4
CPS
MWS-Y
MWS-Z
MWS-X

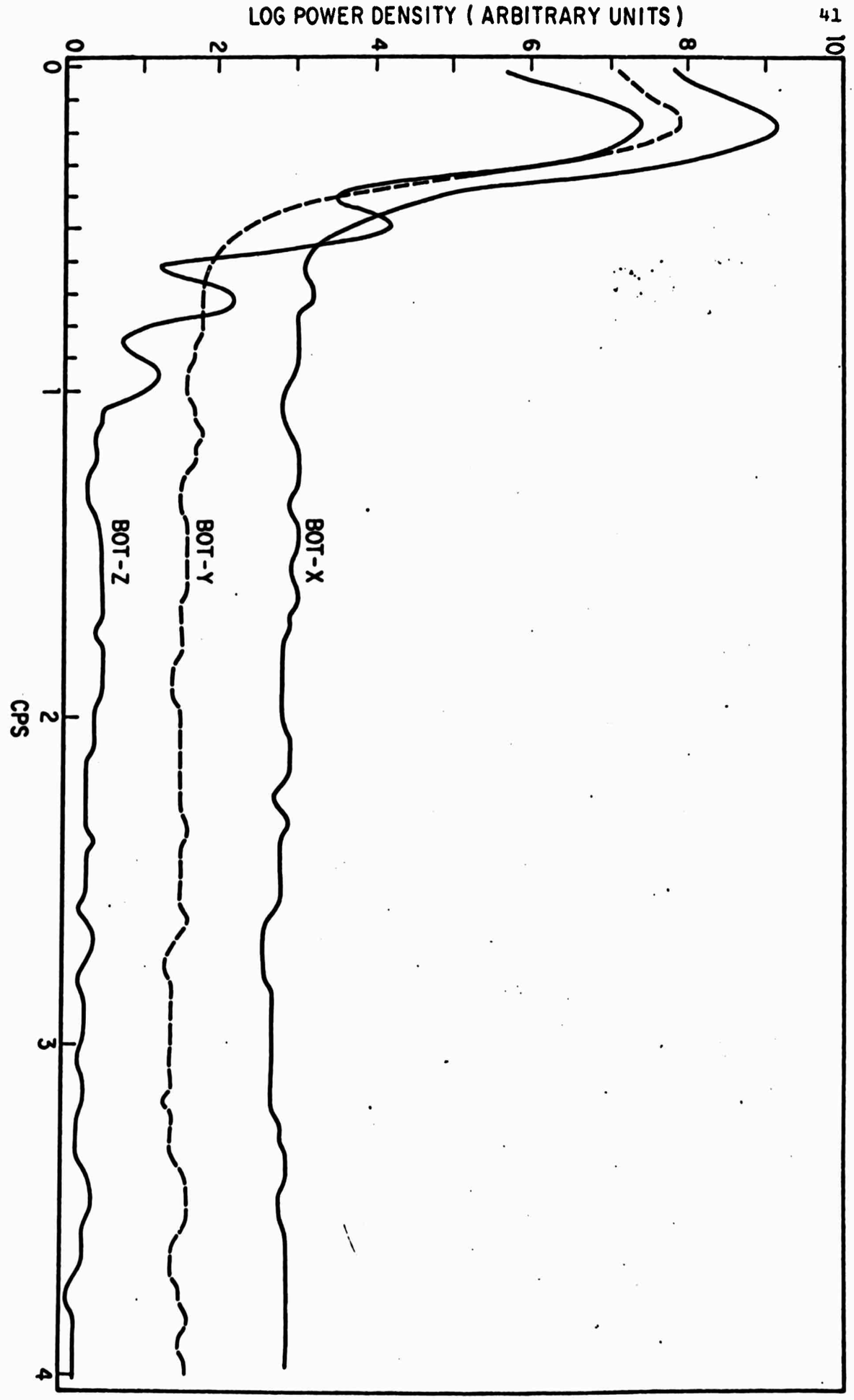
LOG POWER DENSITY (ARBITRARY UNITS)
0
2
4
6
8
10
0
1
2
3
4
CPS
BOT-Z
BOT-Y
BOT-X

Fig. 8

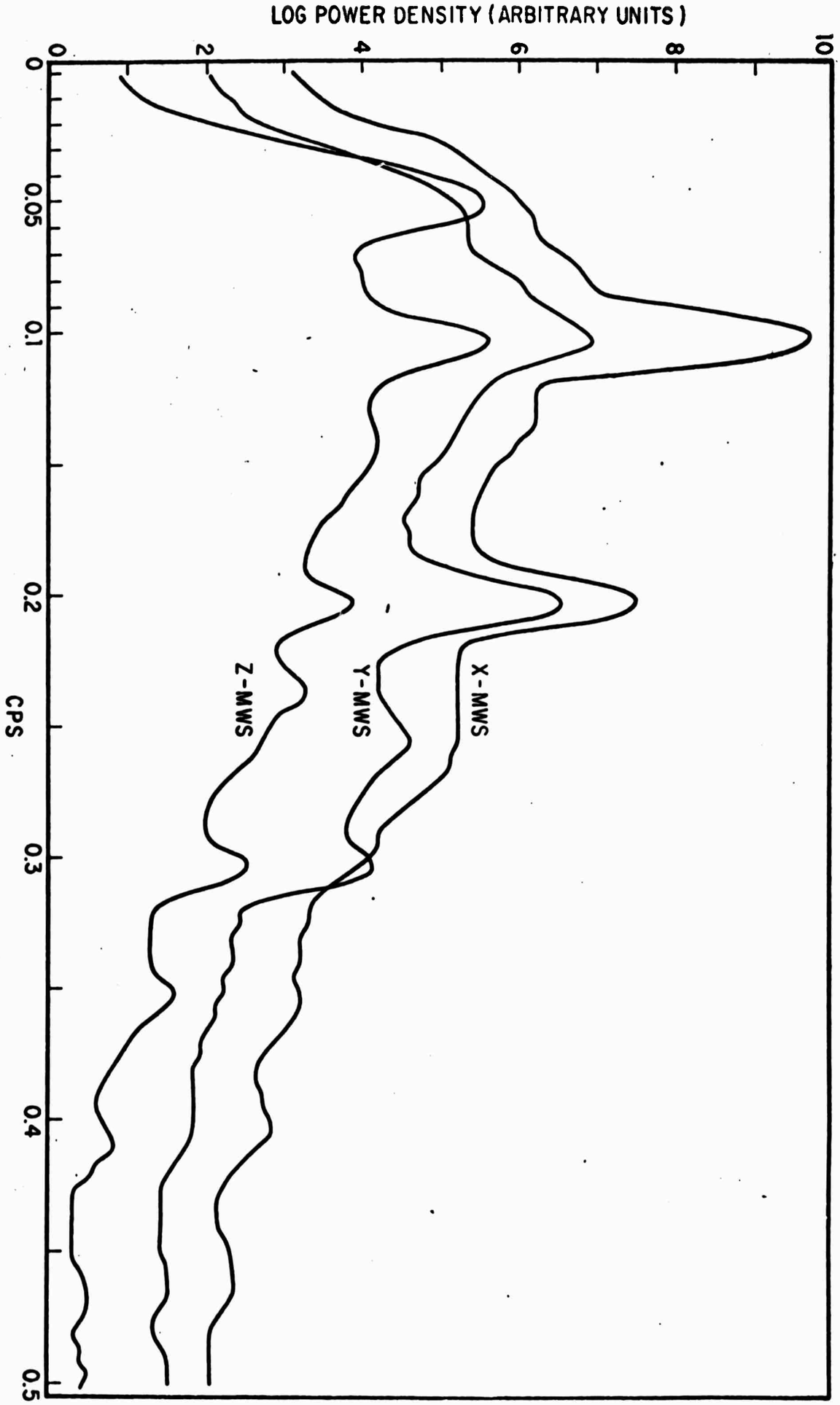
LOG POWER DENSITY (ARBITRARY UNITS)
0
2
4
6
8
10
0
0.05
0.1
0.2
0.3
0.4
0.5
CPS
Z-MWS
Y-MWS
X-MWS

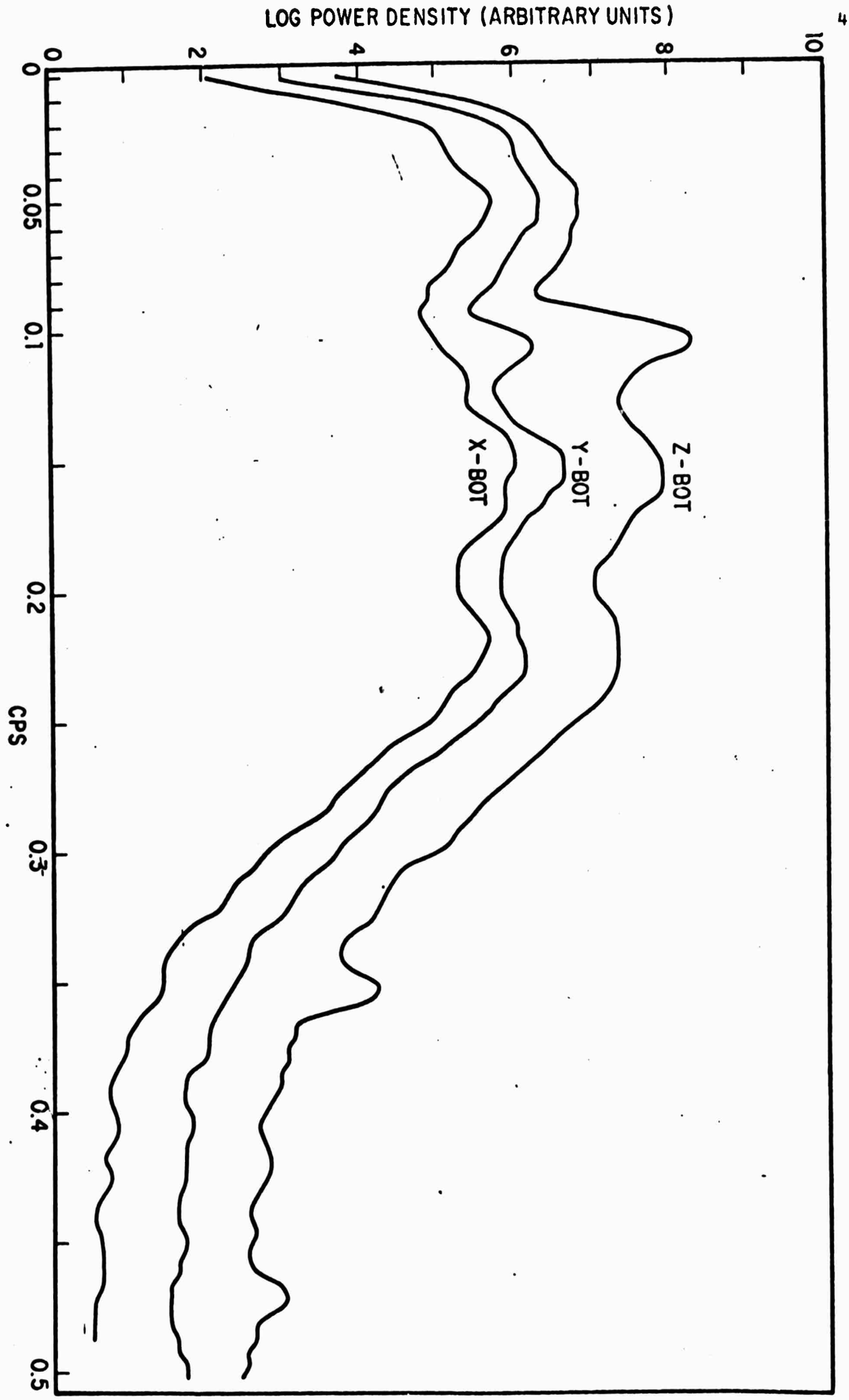
LOG POWER DENSITY (ARBITRARY UNITS)
0
2
4
6
8
10
0
0.05
0.1
0.2
0.3
0.4
0.5
CPS
X-BOT
Y-BOT
Z-BOT

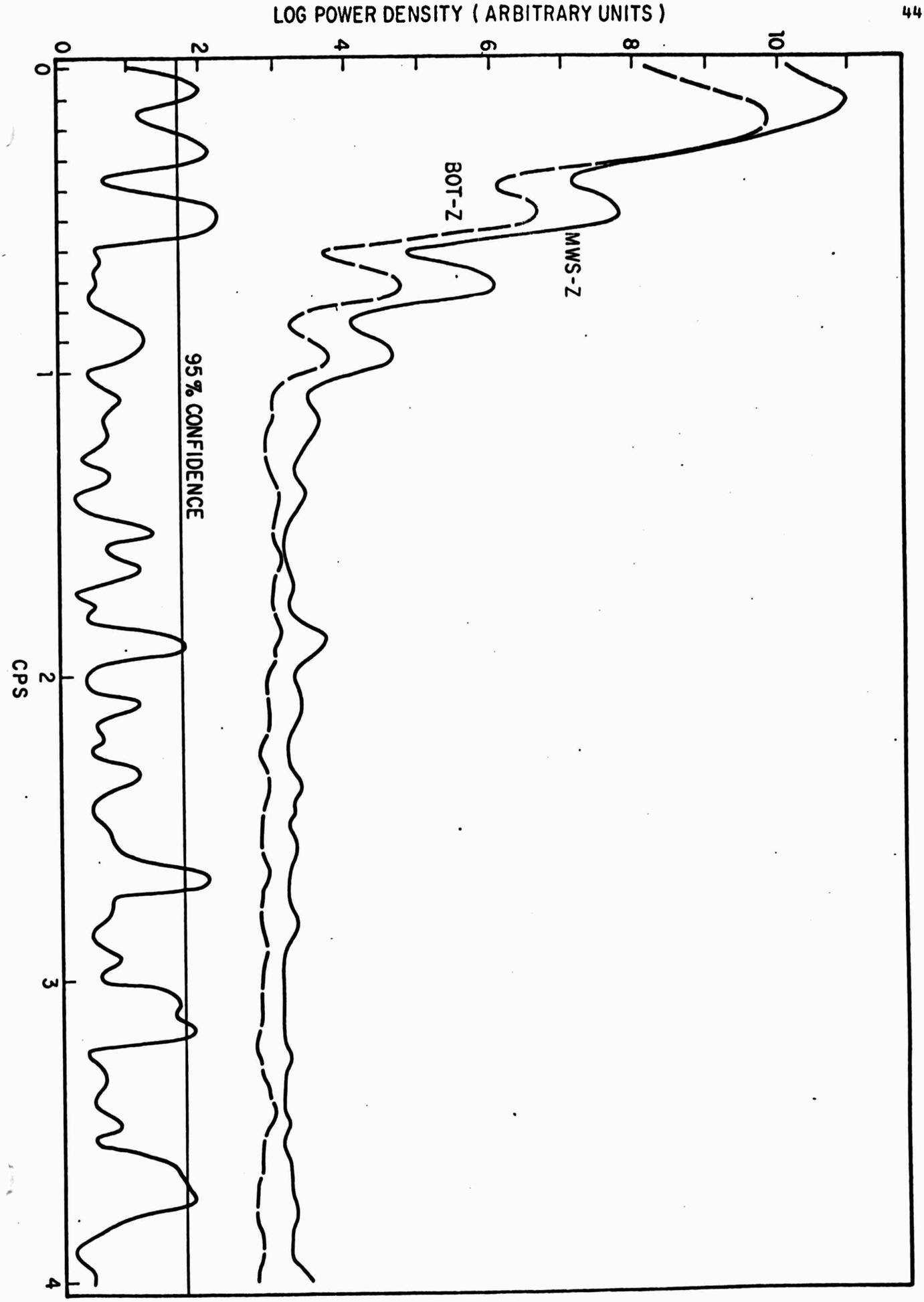
LOG POWER DENSITY (ARBITRARY UNITS)
0
2
4
6
8
10
BOT-Z
MWS-Z
95% CONFIDENCE
0
1
2
3
4
CPS

SEISMIC NOISE BETWEEN 2.5 AND 200 CYCLES PER HOUR

Richard A. Haubrich

ABSTRACT

The seismic background noise between 2.5 and 200 cycles per hour (cph) was measured at TFSO, Payson, Arizona using two instruments, a modified LaCoste gravity meter (LC) and a Geotech vertical seismometer (ZLP1). The spectra of ground acceleration from simultaneous records of the two instruments indicate that ZLP1 is subject to an increasing amount of instrument noise as the frequency decreases below 200 cph. The LaCoste spectrum is considered to represent primarily true ground motion. This spectrum ranges between 10^{-24} and $10^{-23}(\Delta g/g)^2$/cph in the band from 6 to 60 cph. Above 60 cph, the spectrum rises due to storm induced microseisms. Below 6 cph, the spectrum is observed to rise at about 12 db per octive. In spite of the fact that no coherence was observed between atmospheric pressure and ground motion, we suspect that the primary cause of seismic noise below 60 cph is loading due to atmospheric pressure variations.

1. Introduction

Digital recordings of ground motion were made at the Tonto Forest Seismological Observatory (TFSO), Payson, Arizona. The two principal seismic instruments used were a modified LaCoste vertical gravimeter (Block and Moore, 1966) and a Geotech vertical long period seismometer, ZLP1. The Geotech instrument (Model 7505A) was installed in the main vault at TFSO in a room sealed to atmospheric pressure. The LaCoste (LC) instrument was installed in the experimental vault which is located about 1.0 km from ZLP1. In addition some recordings were made with a microbaragraph located near ZLP1. Other long period vertical seismometers were also recorded along with ZLP1 and LC.

Records were chosen for analysis which were free from obvious earthquake surface waves. Results of the spectrum of ground motion and cross spectra between various components are given below.

2. Spectra

Figures 1 and 2 give the instrument response functions for ZLP1 and LC. Zero db represents an output of 1.0 $(lc)^2$ for an input of $10^{-24}(\Delta g/g)^2$ where lc is "least count", the value of one unit in the digital output. A least count change is produced by an input voltage change to the digitizer of .61 millivolts. The unit $\Delta g/g$ is an input to the seismometer of about 10^{-3} gals acceleration where Δg is the acceleration change and g is the value of gravitational acceleration at the earth's surface.

Table 1 gives the data for the three spectra shown in Figures 3, 4 and 5. Each figure shows two spectra calculated from the digital records obtained from the ZLP1 and the LaCoste instruments. The spectra have all been corrected for instrument response.

From the figures, one sees that the ZLP1 spectrum exceeds the LaCoste spectrum as the frequency decreases below 200 cycles per hour. At 200 cph and above (not shown) the two spectra are essentially the same. We conclude from this that the ZLP1 spectrum is due principally to instrument noise at the lower frequencies. The spectrum of ZLP1 rises at about 6 to 9 db per octave toward low frequency. If we assume that the noise source is the displacement of the seismometer mass with respect to its supports, then the moving coil transducer would produce a 6 db per octave increase with decreasing frequency. If in addition, the ZLP1 amplifier is subject to 1/f noise below 50 cph, this would explain the 9 db per octive slope in Figures 3 and 4.

Recordings were also made of ZLP2 and ZLP7 from the TFSO

seismic array. The final corrected spectra of ground motion from these were found to be no lower (and often higher) than that obtained from ZLP1. The spectrum from the LaCoste instrument shows a consistent low level between 6 and 100 cycles per hour. The spectral density in this band varies as a function of frequency and time by about 10 db. The lowest level observed is $10^{-24}(\Delta g/g)^2$/cph (Figure 3).

The LaCoste meter has a theoretical thermal noise level of about $5 \times 10^{-25}(\Delta g/g)^2$/cph. We feel that the actual instrument noise level is close to this so that the lowest level of the observed spectrum represents about 50% ground motion and 50% instrument noise. The observed spectrum increase below 6 cph is considered to be a property of seismic noise.

Table 2 gives a conversion of units from $(\Delta g/g)^2$/cph to displacement in cm and time in seconds for two frequencies, 10 cph and 60 cph. Column 3 gives the values of displacement spectrum density in urits of $(cm)^2$ sec for our zero db level of $10^{-24}(\Delta g/g)^2$/cph. Column 4 gives the rms value of ground displacement in cm for a band one octive wide centered at 10 and 60 cph. Thus the lowest level of ground motion measured with the LaCoste would produce a trace amplitude with less than 1 cm rms when played through an octive filter at 60 cph with a magnification of 10^6. The lowest level at 10 cph which is somewhat above 0 db (Figure 4) would give about 1 cm rms at a magnification of 10^5.

3. Cross Spectra

The cross spectrum was computed between ZLP1 and the LaCoste records. As an example, for the data of Figure 4, the coherence drops from a value of .99 at 200 cph down to near zero at 100 cph and is essentially zero at frequencies below 100 cph. Small coherences are to be expected below 100 cph if we assume that ZLP1 is noisy.

Consider the case at 120 cph; the coherence estimate is 0.4. Let S represent the spectrum of propagating seismic noise. The coherence γ between two stations 1 km. apart is essentially 1.0 for S. Let S_1 and S_2 be the instrument noise spectra for ZLP1 and LC. Let S_n be the spectrum of high wave number ground motion which is the same at both ZLP1 and LC. Then we have

$$\gamma = \frac{S^2}{(S + S_1 + S_n)(S + S_2 + S_n)}$$

The spectra of ZLP1 and LC give

$$S + S_2 + S_n = \frac{1}{1.6}(S + S_1 + S_n) = S_t = 7.1 \times 10^{-24}\left(\frac{\Delta g}{g}\right)^2/\text{cph}$$

The two equations give

$$\frac{S_n}{S + S_n} = \frac{.2S_t - S_2}{S_t - S_2}$$

If we take $S_2 = 5 \times 10^{-25}(\frac{\Delta g}{g})^2/\text{cph}$ then $\frac{S_n}{S + S_n} = .14$ so that about 1/7 of the power is high wave number noise. This value depends on the assumed value of S_2 . If $S_2 = 10^{-24}(\frac{\Delta g}{g})^2/\text{cph}$, than $S_n/(S+S_n) = .07$.

Cross spectra were also computed between the microbaragraph and ZLP1 and LC. No significant coherence was found between the seismic and the barograph data at any frequencies between 2 and 200 cph. The lack of coherence does not necessarily mean that the ground motion below 100 cph is unrelated to atmospheric pressure changes. On the contrary, the evidence suggests that the low level spectrum observed on the LC could be atmospherically induced.

Consider the following model of atmospheric pressure loading. A homogeneous half space with Lamé parameters λ , μ is loaded by constant pressure p_o over a sector bounded by polar coordinates $r_1 \leq r \leq r_2$; $\theta_1 \leq \theta \leq \theta_2$. At the origin the vertical ground displacement due to the static load is given by

$$w_o = \frac{C}{2\pi} p_o(r_2 - r_1)(\theta_2 - \theta_1)$$

$$C = \frac{\lambda + 2\mu}{2\mu(\lambda + \mu)}$$

Divide the plane by circles concentric with the origin such that each circle has radius

$$R_n = (2n - 1)R \quad ; \quad n = 1, 2, 3...$$

where R is a scale length. If

$$A = \pi R^2$$

is the area of the central circle, then each ring $R_{n-1} \le r \le R_n$ has area

$$A_n = 8(n-1)A \quad ; \quad n = 2, 3, \ldots$$

Divide each ring into $8(n-1)$ equal area sectors by drawing radii at intervals of $\theta = 2\pi/8(n-1)$ in each ring. The plane has now been sectored into equal area regions, each approximately square.

Our model is that each of the sectors is loaded by atmospheric pressure variations independent of all the others and that p_o has the same mean square value (in time) for each sector. The spectrum of w_o (which we designate as $\langle w_o^2 \rangle$) will thus be the sum of the spectra from each sector. We assume that the pressure wave lengths are small compared to seismic wave lengths so that the static loading theory holds. The contribution in power due to the central circle is proportional to R^2. The contribution from all the sectors in the n^{th} ring is

$$8(n-1)\left[\frac{2R}{8(n-1)}\right]^2 = \frac{R^2}{2(n-1)} \quad ; \quad n = 2, 3, \ldots$$

so that the total power is proportional to

$$R^2\left[1 + \frac{1}{2} S_n\right]$$

where $S_n = 1 + \frac{1}{2} + \frac{1}{3} + \ldots \frac{1}{n}$.

is the harmonic series. As n goes to infinity, S_n diverges; but it doesn't diverge very fast. For $n = 1{,}000$, $S_n = 7.5$ while for $n = 30{,}000$, $S_n = 10.9$.

Letting $\lambda = \mu = 2 \times 10^{11}$ dynes/cm^2 we have

$$R^2(1 + \tfrac{1}{2} S_n) = 7.1 \times 10^{22} \frac{\langle w_o^2 \rangle}{\langle p_o^2 \rangle}$$

Consider the frequency 60 cph; taking $\langle w_o^2 \rangle = 3 \times 10^{-11}$ cm^2 sec ((Table 2) and $\langle p_o^2 \rangle = 10^3$ (dynes/cm)^2 sec (Haubrich and MacKenzie, 1965).

$$R(1 + \tfrac{1}{2} S_n)^{\frac{1}{2}} = 460 \text{ meters}$$

from which R is determined for a given . Thus for

$n = 1{,}000$	$R = 211$ meters
$n = 30{,}000$	$R = 182$ meters

For n larger than 1000 the model is rather insensitive to the value of n .

From this model, we conclude that the coherence between pressure induced ground motion and local pressure should be $1/(1 + \frac{1}{2} S_n)$ which is about .21 at $n = 1000$ and .15 at $n = 30{,}000$. These coherence values are too low to be observed from the data considered here.

The values of R obtained are close to those observed for cases where coherent pressure and ground motion were observed (Haubrich and MacKenzie, 1965). On those occasions when the observed coherence is above 0.5, one must assume that the above model fails in that $\langle p_o^2 \rangle$ is higher than average in the areas close to the seismometer.

As frequency decreases, the pressure spectrum typically increases by about 9 to 12 db per octive. This explains the relatively flat ground acceleration spectrum above 6 cph. The increase in the ground spectrum at lower frequencies would seem to indicate that R increases with the period of atmospheric pressure variations below 6 cph.

.eferences

Block, B. and R. D. Moore, Measurements in the earth mode frequency range by an electrostatic sensing and feedback gravimeter, *J. Geophys. Res., 71,* 4361 - 4375, 1966.

Haubrich, R. A. and G. S. MacKenzie, Earth noise, 5 to 500 millicycles per second: 2. Reaction of the earth to oceans and atmosphere, *J. Geophys. Res., 70,* 1429 - 1440, 1965.

TABLE 1

Figure No.	Date	Start Time MST	Sample Rate	Record Length
3	4/17/69	1320	$3\frac{1}{8}$/sec.	2.9 hr.
4	4/18/69	1040	$3\frac{1}{8}$/sec	7.3 hr.
5	8/16/69	1200	$3\frac{1}{8}$/sec	2.9 hr.

TABLE 2

cph	Period Seconds	$10^{-24}(\Delta g/g)^2$/cph	$10^{-24}(\Delta g/g)^2$/cph
10	360	3.9×10^{-8} cm^{2}sec	8.7×10^{-6} cm rms/octive
60	60	3.0×10^{-11} cm^{2}sec	5.9×10^{-7} cm rms/octive

Figure 1: Response of ZLP1 in db relative to $1.0(1c)^2$ per $10^{-24}(\Delta g/g)^2$.

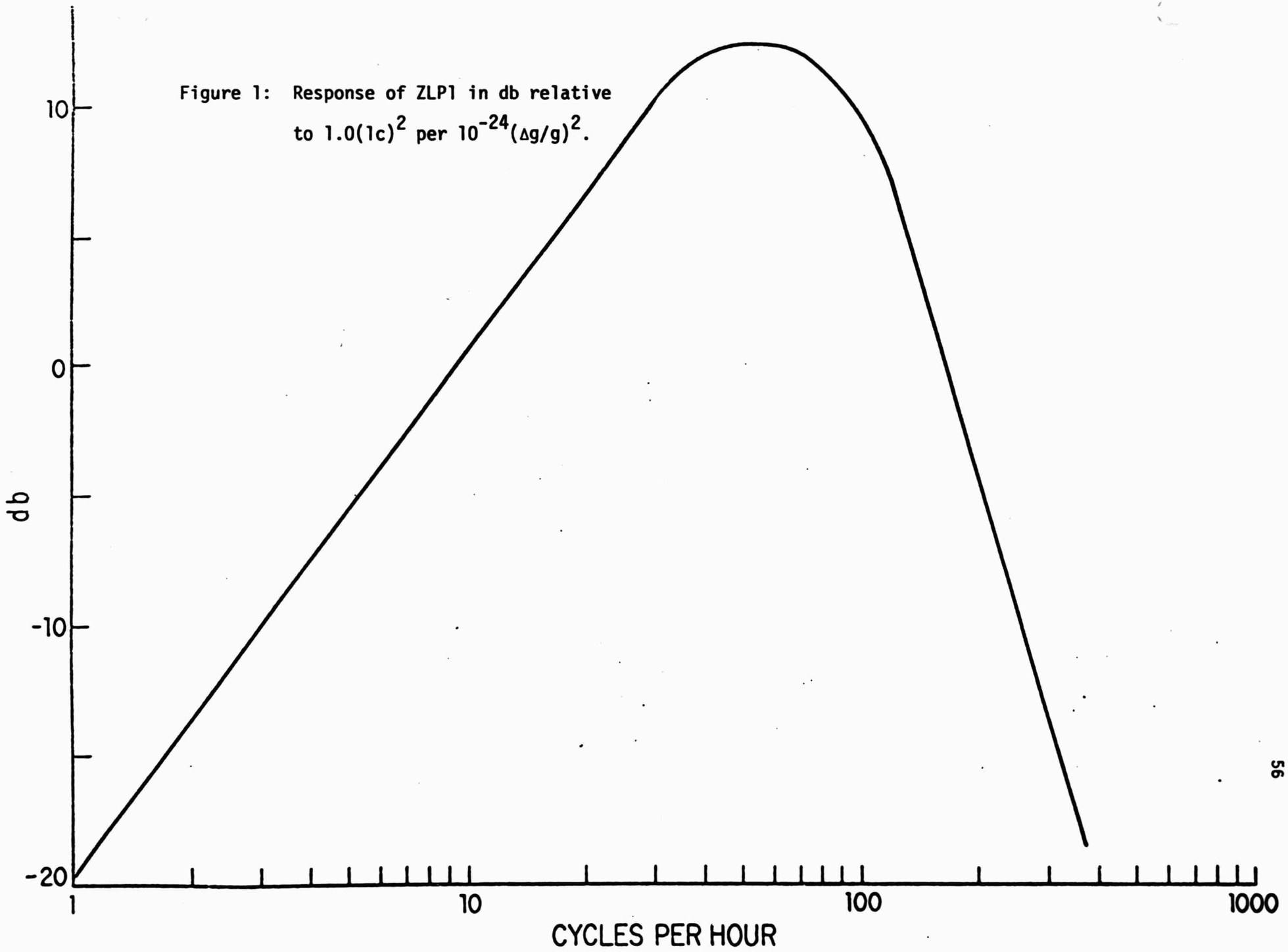

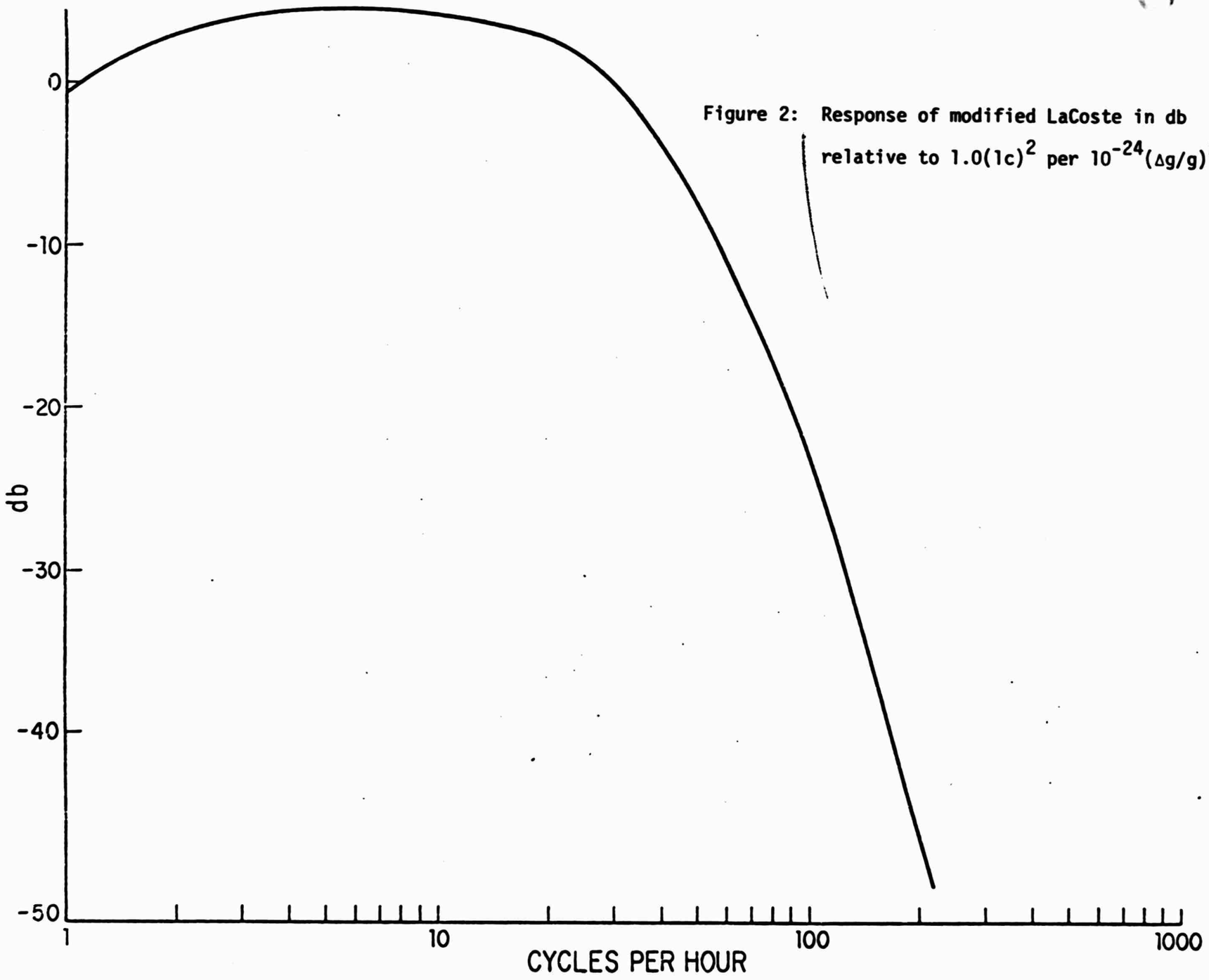

Figure 2: Response of modified LaCoste in db relative to $1.0(1c)^2$ per $10^{-24}(\Delta g/g)^2$.

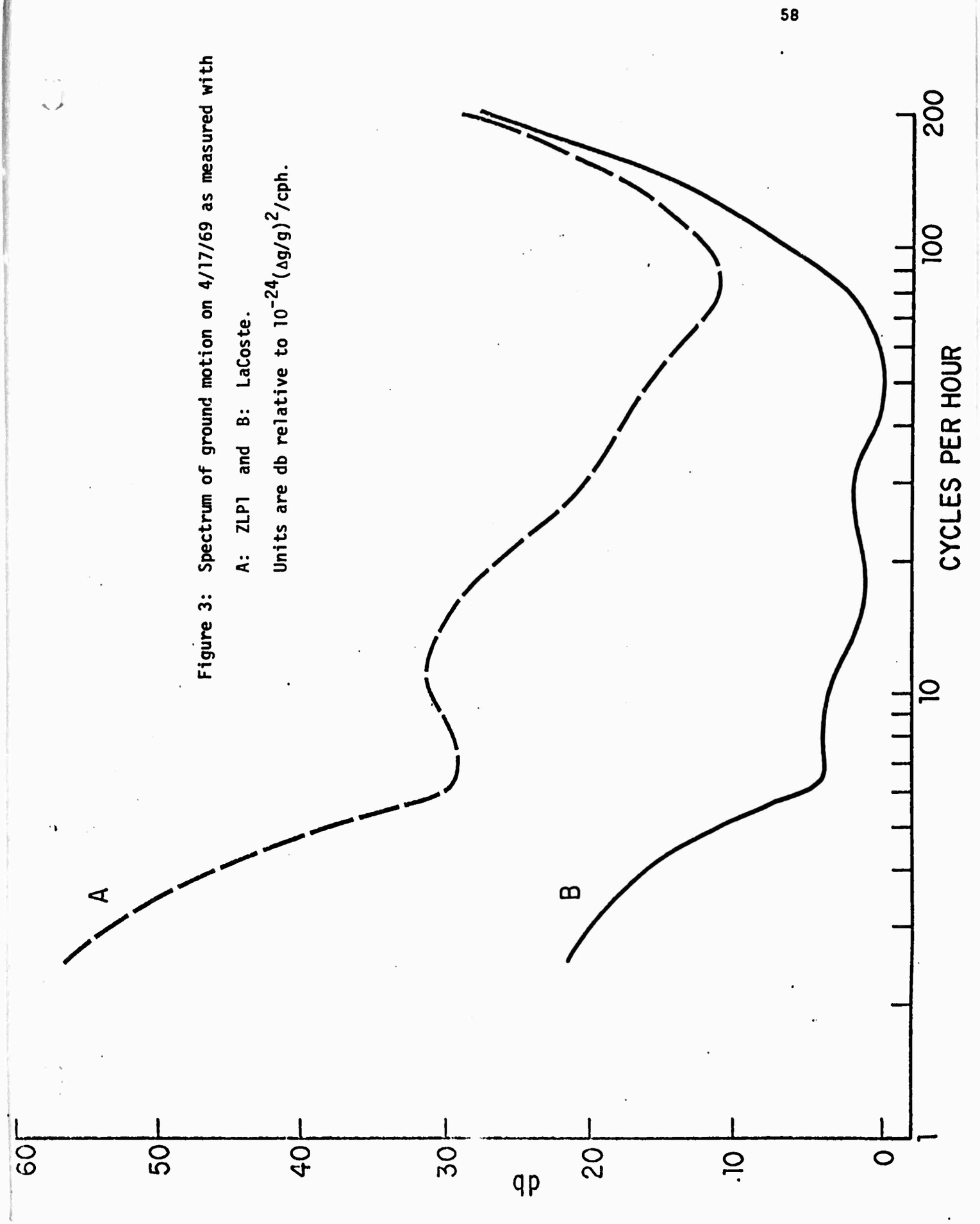

Figure 3: Spectrum of ground motion on 4/17/69 as measured with
A: ZLP1 and B: LaCoste.
Units are db relative to $10^{-24}(\Delta g/g)^2$/cph.

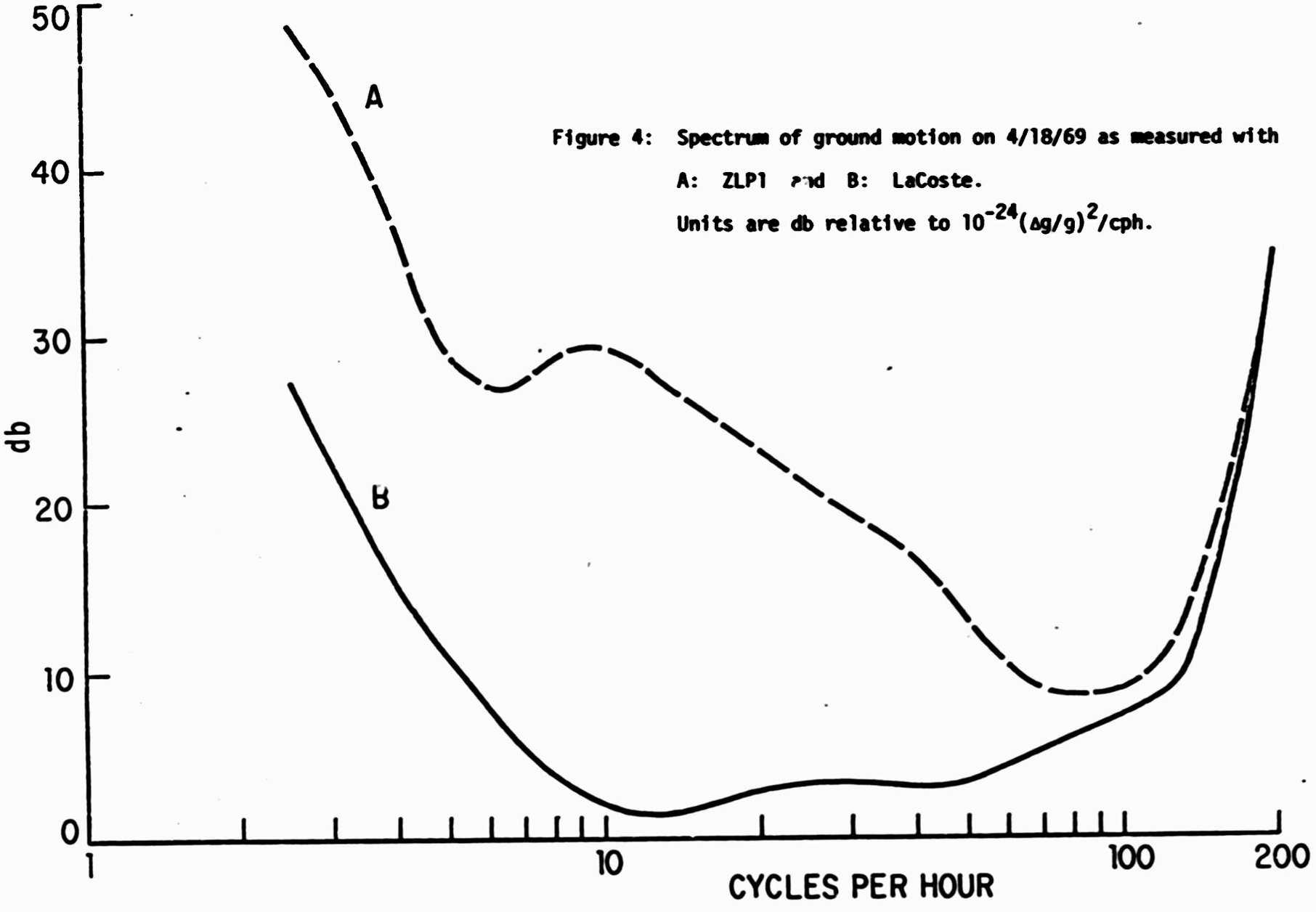

Figure 4: Spectrum of ground motion on 4/18/69 as measured with A: ZLP1 and B: LaCoste.
Units are db relative to $10^{-24}(\Delta g/g)^2$/cph.

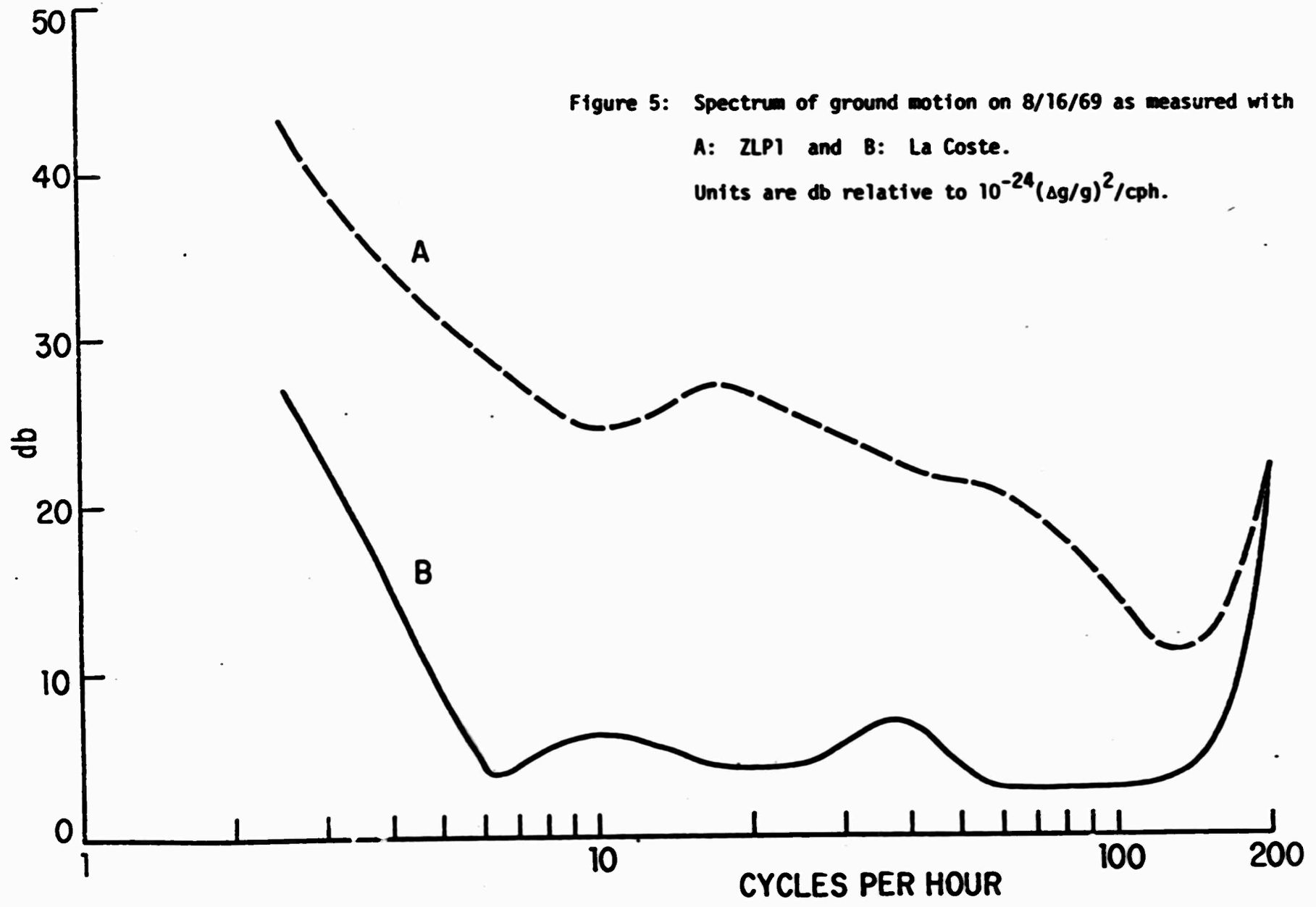

Figure 5: Spectrum of ground motion on 8/16/69 as measured with A: ZLP1 and B: La Coste.
Units are db relative to $10^{-24}(\Delta g/g)^2$/cph.

LINEARIZATION AND CALIBRATION OF ELECTROSTATICALLY FEDBACK GRAVITY METERS

By Robert D. Moore and W. E. Farrell

Abstract

One of the common techniques for converting LaCoste-Romberg survey gravity meters into fedback continuously recording tidal gravity meters is to detect the mass position with a capacitor bridge and apply feedback forces electrostatically. In general, this servosystem is nonlinear and the output voltage has a quadratic as well as a linear dependence on gravity. For the tidal variation in gravity, the quadratic term can be reduced from typically 10% to .1% of the linear term with a modification of the standard feedback system. The linearized, fedback gravity meter is precisely calibrated by a two-step procedure. First, the tilt method is used to determine the zero frequency response. The frequency dependence of the transfer function, vital for accurate phase calibration at tidal frequencies, is measured by inserting a random signal in the feedback loop and crosscorrelating the random signal with the gravity meter output. The accuracy of the calibration at tidal frequencies is ± .3% in amplitude and ± .2 degrees in phase.

J. Geophys. Res., *75*, 928-932, 1970

UNCLASSIFIED

Security Classification

DOCUMENT CONTROL DATA - R & D

(Security classification of title, body of abstract and indexing annotation must be entered when the overall report is classified)

1 ORIGINATING ACTIVITY (Corporate author) University of California, San Diego Institute of Geophysics and Planetary Physics La Jolla, California	2a. REPORT SECURITY CLASSIFICATION UNCLASSIFIED 2b. GROUP

3 REPORT TITLE

Low Level Earth Motion

4 DESCRIPTIVE NOTES (Type of report and inclusive dates)

Final Report - 1 May 1964 - 30 Sep 1969

5 AUTHOR(S) (First name, middle initial, last name)

Richard A. Haubrich

6 REPORT DATE 1 May 1970	7a. TOTAL NO. OF PAGES 66	7b. NO OF REFS 14
8a. CONTRACT OR GRANT NO AF49(638)-1388 b. PROJECT NO 8652 c. 62701D d.	9a. ORIGINATOR'S REPORT NUMBER(S) 9b. OTHER REPORT NO(S) (Any other numbers that may be assigned this report) AFOSR 70-1693 TR	

10 DISTRIBUTION STATEMENT

1. This document has been approved for public release and sale; its distribution is unlimited.

11 SUPPLEMENTARY NOTES TECH, OTHER	12 SPONSORING MILITARY ACTIVITY AF Office of Scientific Research (SRPG) 1400 Wilson Boulevard Arlington, VA 22209

13 ABSTRACT

1. A scheme recently proposed by the authors for constructing Earth models which fit a given finite set of gross Earth data is applied to the problem of constructing a P-velocity structure which, within experimental error, fits the observed travel times in the range $\Delta + 25^{\circ}(5^{\circ})95^{\circ}$. Three such models are obtained, all of which fit the observed travel times with residuals less than 0.06^{s}, whereas 0.5^{s} is the estimated standard error of the observations. The models differ mainly in the outer 700 km of the mantle.

2. A gross Earth datum is a single measurable number describing some property of the whole Earth, such as mass, moment of inertia, or the frequency of oscillation of some identified elastic-gravitational normal mode. We suppose that a finite set of G of gross Earth data has been measured, that the measurements are inaccurate, and that the variance matrix of the errors of measurement can be estimated. We show that some such sets G of measurements determine the structure of the Earth within certain limits of error except for fine-scale detail. That is, from some sets G it is possible to compute localized average of the earth structure at various depths. These localized averages will be slightly in error, and their errors will be larger as their resolving lengths are shortened. We show how to determine whether a given set G of measured gross Earth data permits such a construction of localized averages and if so, how to find the shortest length scale over which G gives a local average structure at a particular depth if the variance of error in computing that local average from G is to be less than a specified amount.

DD FORM 1 NOV 65 1473

UNCLASSIFIED

Security Classification

14. KEY WORDS	LINK A		LINK B		LINK C	
	ROLE	WT	ROLE	WT	ROLE	WT
Mode theory						
Resolving Power						
Gross earth Data						
Q						